District Geologist, Smithers   Off Confidential: 94.11.24

ASSESSMENT REPORT 23289   MINING DIVISION: Omineca

PROPERTY: Whiting
LOCATION: LAT   53 45 00   LONG   127 10 00
               UTM   09 5957050   620891
               NTS   093E11E   093E14E
CLAIM(S):   Whit 1-6,Whit Fr.
OPERATOR(S):   New Camamin Res.
AUTHOR(S):   Somerville, R.
REPORT YEAR: 1994, 73 Pages
COMMODITIES
SEARCHED FOR: Molybdenum/Molybdenite,Copper,Gold,Silver
KEYWORDS: Jurassic,Takla Group,Granodiorites,Quartz porphyry,Monzonites
               Chalcopyrite,Porphyry copper,Molybdenite,Pyrite
WORK
DONE: Geophysical
           EMAB   575.0 km;VLF ,REST
               Map(s) - 6; Scale(s) - 1:10 000
           MAGA   575.0 km
               Map(s) - 8; Scale(s) - 1:10 000
           RADA   575.0 km
               Map(s) - 8; Scale(s) - 1:10-000
MINFILE: 093E 049,093E 050,093E 113

RSGM R. Somerville Geological & Mining Engineering Ltd.

Suite 240 - 171 West Esplanade • North Vancouver, B.C. Canada V7M 3K9 • Tel: (604) **986-5766** Fax: (604) 986-5928

VOLUME I

AIRBORNE GEOPHYSICAL REPORT

ON THE

WHIT 1 to 6 MINERAL CLAIMS

WHITING CREEK PROPERTY

Omineca Mining Division, British Columbia
NTS 93E/11E & 14E
Latitude 53°45'N
Longitude 127°10'W

on behalf of

NEW CANAMIN RESOURCES LTD.
&
KENNECOTT CANADA INC.

by

Richard Somerville, P.Eng., F.G.A.C.
R.SOMERVILLE GEOLOGICAL & MINING ENGINEERING LTD.
#240 - 171 West Esplanade
North Vancouver, B.C.
V7M 3K9

January 15, 1994

GEOLOGICAL BRANCH
ASSESSMENT REPORT

PART 1 OF 2 23,289

TABLE OF CONTENTS

Page No.

LIST OF FIGURES

Page No.

IN VOLUME II (MAPS)

INTRODUCTION

SUMMARY

Between July 2nd and July 7th an airborne survey was flown over Areas A North and A South.(see Index Map #3) The Whiting Creek copper deposits underlie Area A North and the Huckleberry deposits underlie Area A South. The objective of this survey was to identify an airborne geophysical model for the known deposits and to use this model to identify any other porphyry copper/molybdenum targets on either property. The airborne total field magnetic survey is moderately successful in identifying magnetically high Bulkley intrusives and the Huckleberry Main and East zones are fairly well indicated by magnetic lows and VLF-EM conductive peaks flanking the intrusives. To a greater or lesser extent the apparent resistivity, total field VLF-EM, and vertical magnetic gradient all seem to indicate a complex pattern of NW and NE striking linear structures (mainly faulting) in the area flown. A number of areas appear to have geophysical characteristics similar to those of the known mineralized areas.

Respectfully Submitted

R. Somerville P.Eng.
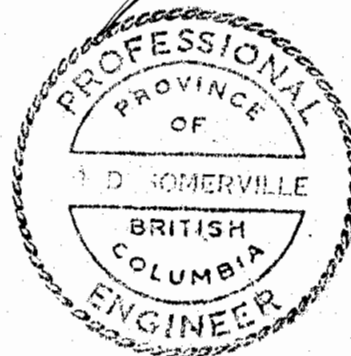
LOCATION, PHYSIOGRAPHY, ACCESS

The WHITING CREEK property is situated approximately 80 kilometres south-southwest of Houston, B.C. (Figures 1 & 2). The claim group lies about 15km north of Tahtsa Reach and approximately 47 air kilometres north-northeast of Kemano, B.C. on the south slope of Sibola Mountain. The NTS map sheet number is 93E/11E-14E and the latitude and longitude is as follows:

LATITUDE: 53 45'N
LONGITUDE: 127 13'W

The property can be reached by a total of 125 km of good gravel road which are currently being used as mainline logging access roads. A rough four-wheel drive road for about 8 km leads from the logging road to areas of interest above treeline in the Whiting Creek and Rusty Creek valleys. A route log for access to the property is as follows:

1.) From Highway 16 just north of Houston turn west on the Morice River Road to the junction with the Morice Owen Road.
2.) Follow the Morice Owen Road to the Nadina Road
3.) Follow the Nadina Road to the Tahtsa Road
4.) Follow the Tahtsa Road to the Whiting Creek Road (immediately north of Sweeney Lake)
5.) Follow the Whiting Creek Road north onto the property.

Sweeney Lake has an elevation of about 940 metres asl, and elevations on the property range up to 2,190 metres. The topography is very rugged, especially on the north half of the claims. The treeline occurs at approximately 1,500 metres elevation.

The property lies at the north end of the Boundary Ranges of the Coast Mountains. Moderately steep mountain slopes, broad U-shaped valleys, large narrow northeast-trending lakes draining ice-fields and glaciers to the west, are the dominant physiographic features of the area. Slopes on the property are steep. Glaciers have scoured the valley walls leaving a shallow

overburden on the tops of the ridges and infilling the valleys with glacialfluvial gravels and sandy clay. Between the lake level at 940 and about 1,500 metres, slopes are heavily covered with slide alder, mountain ash, willow, huckleberry, false azalea and gnarled spruce, balsam fir and alpine fir. Occasional spruce, hemlock and pine also have been observed. Above 1500 metres, (the treeline) the area is mainly covered by talus with colourful red and yellow gossans.

Whiting and Rusty Creek flow most of the year but can be intermittent in a dry year. Rusty Creek joins Whiting Creek and it eventually flows into Tahtsa Reach.
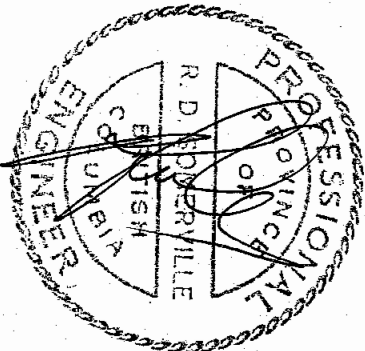
Location Map
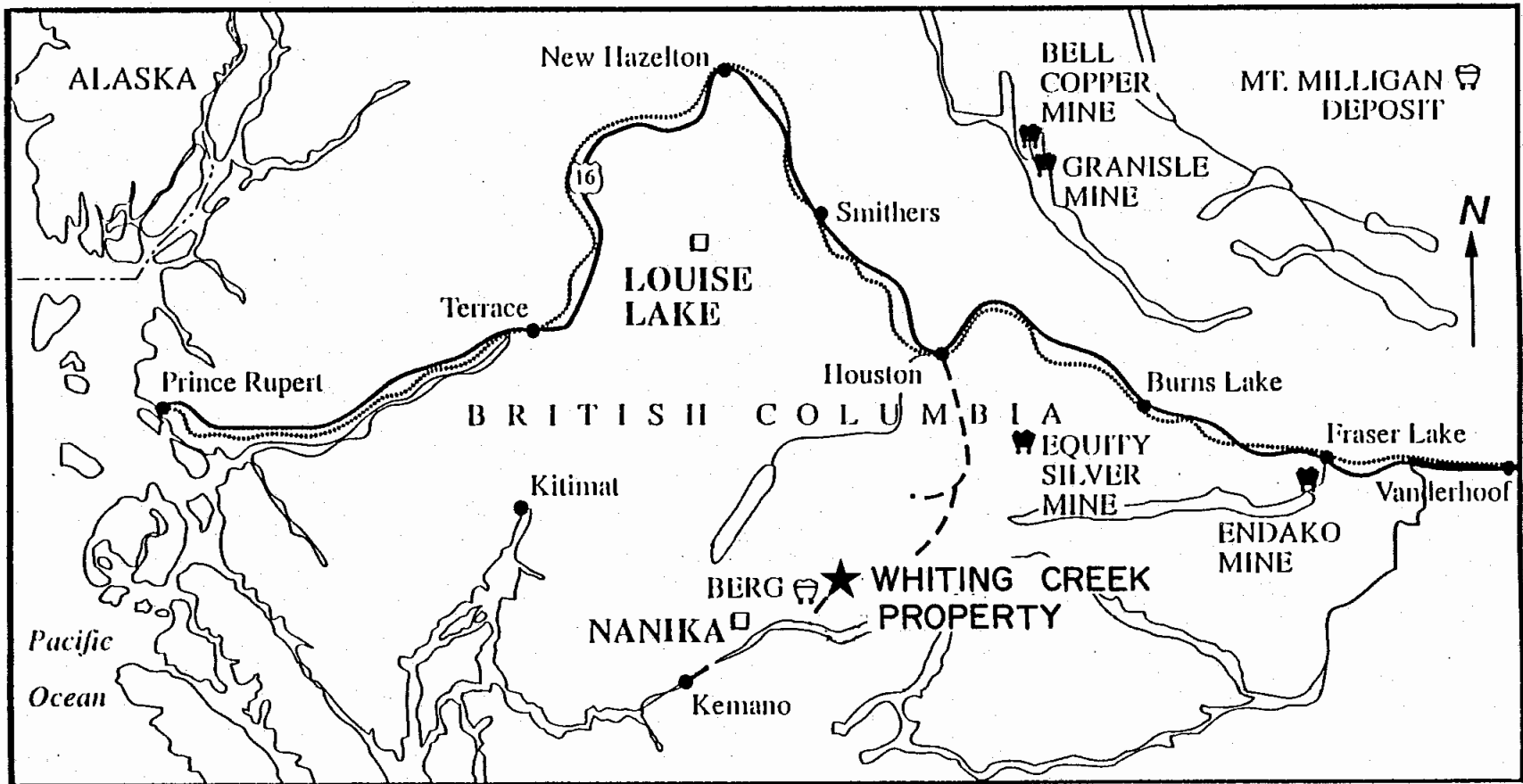
NEW CANAMIN RESOURCES LTD. Whiting Creek Property, B.C.

├─── 100kms ───┤

FIG.1

NEW CANAMIN RESOURCES LTD.
WHITING CREEK PROPERTY
PROJECT CLAIM MAP

(Taken from MEMPR Mineral Titles
Reference Maps 93E11E, 93E14E)

FIGURE: 2
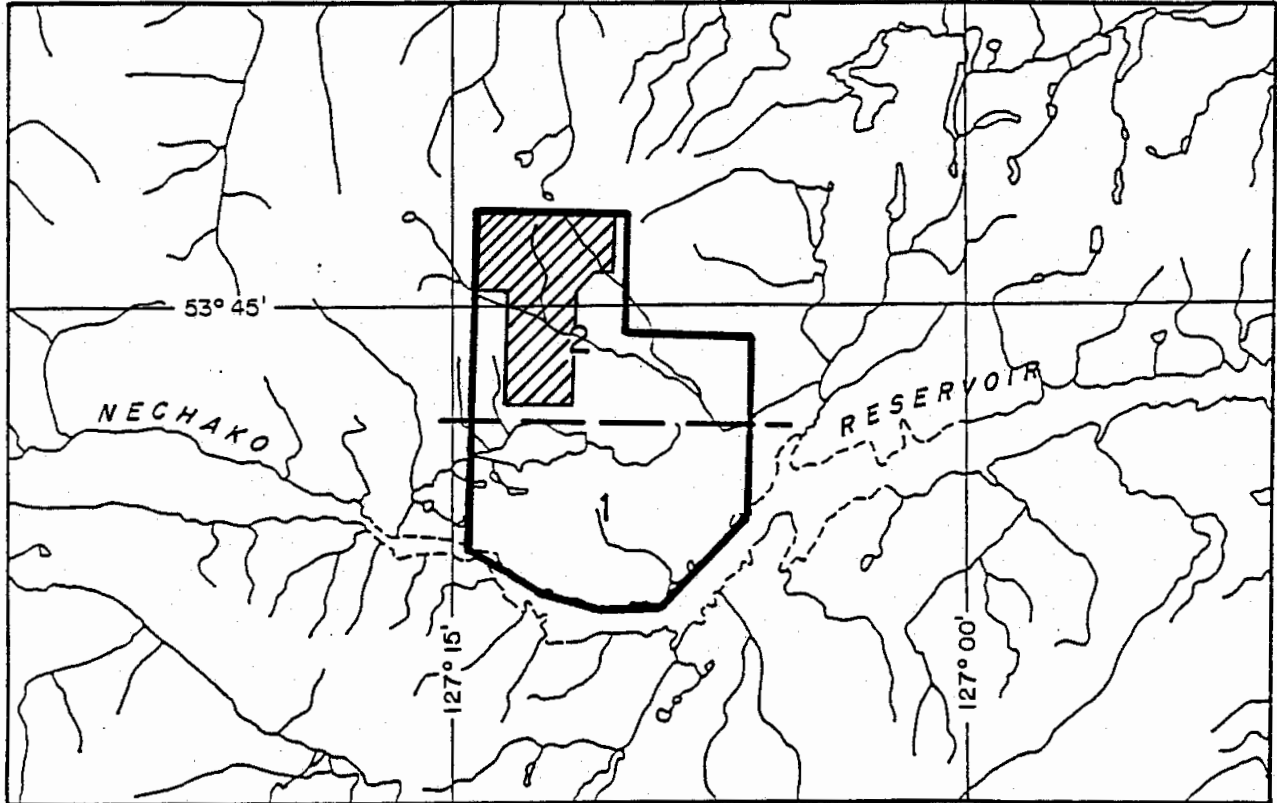
INDEX MAP #3

NTS 93E11

2-AREA A NORTH

1-AREA A SOUTH

-WHITING CREEK PROPERTY

SURVEY AREA

WHITING CREEK PROPERTY

AIRBORNE GEOPHYSICAL WORK COMPLETED IN 1993

Between July 2nd and July 7th, an airborne survey was flown over Areas A North and A South. (see Index Map #3) The Whiting Creek Property is covered by the survey over Area A North.

A report by R. W. Woolham, P.Eng. Consulting Geophysicist, is included in this report in Appendix #1. Mr. Woolham describes in his report survey procedures, instrumentation, data presentation, survey results and conclusions. All the data received from the survey is presented on a series of twenty-two maps, listed in the Table of Contents and located in Volume II of this report.

TENURE AND OWNERSHIP

The WHITING CREEK property comprises 83 claim units which were held in the name of Kennecott Canada Inc. until November 1993 at which time New Canamin Resources Ltd. assumed 100% ownership, subject to a contractual right allowing Kennecott to back-in for a 60% ownership.

The property was originally staked by Kennco Explorations Ltd. in 1963 as the Whit 1-40MC. Subsequently, in 1979, during a joint venture with SMD, the property was abandoned and re-staked as Whit 1-6MC. Whit 17fr was added in 1981.

The claim status at the Whiting Creek property is as follows:

(see Figure 3):

Claim Name	Record No.	No. of Units	Date Staked	Expiry
WHIT 2	238209	20	Nov. 29, 1979	1993
WHIT 1	2569	20	Nov. 29, 1979	1997
WHIT 3	2568	15	Nov. 29, 1979	1997
WHIT 4	3254	15	Nov. 29, 1979	1997
WHIT 5	3255	6	Nov. 29, 1979	1997
WHIT 6	3256	6	Nov. 29, 1979	1997
Whit 17fr	238469	1	August 7,1981	1994

GEOLOGY

REGIONAL GEOLOGY

The Whiting Creek Property is underlain by the middle Jurassic Hazelton Group, a complex group of sedimentary and volcanic rocks which comprise an island arc complex. The complex lies west of the successor Bowser Basin of the intermontane Tectonic Belt and east of the Coast Plutonic Complex. Regionally the Hazelton rocks are in places unconformably overlain by sediments of the Bowser Group. The Hazelton Group is mainly an island arc complex of sub-aerial volcanics of differentiated andesitic to dacitic calc-alkaline composition with interbedded sedimentary facies. The Jurassic rocks are all capped by Skeena marine basin turbidites of Early Cretaceous age, as well as Late Cretaceous age felsic pyroclastics and even later basalt flows, both of the Kasalka Group.

Subsequent to the sedimentary and volcanic activity, the rocks have been complexly folded and faulted and intruded by a succession of small to medium sized intrusives whose ages range from Upper Cretaceous to Eocene. The Eocene Nanika intrusives are known to have porphyry showings, including the Berg copper deposit. However, of these many intrusives, the Late Cretaceous Bulkley Valley hornblende-biotite diorites appear to contain the most important porphyry copper-molybdenum deposits of the district - including the Huckleberry and Whiting Creek deposits.

The regional metamorphic grade is of the lower greenschist facies. The regional scale alteration assemblage consists of moderate chloritic alteration with trace to minor disseminated pyrite. This regional metamorphic event peaked during the mid-Cretaceous time (approximately 110 - 90 Ma). In the immediate vicinity of ore deposits and economic showings a pervasive alteration comprising silica-carbonate-sericite/clay-pyrite is common. This alteration appears to have preceded, accompanied, and

followed, sulphide deposition probably along long-lived or reactivated channel within the stratovolcano. Commonly, accompanying the porphyry sulphide mineralization, are areas of intense to moderate biotization and albitization.

PROPERTY GEOLOGY

The four known Whiting Creek copper-molybdenum deposits are associated with the emplacement of a series of intrusives in the Takla Group volcanics: granodiorite, followed by aplitic quartz porphyry, followed in turn by quartz monzonite porphyry and associated monzonites and finally a late stage hornblende-biotite intrusive stocks and associated andesite dykes. The Ridge and Rusty zones sulphide mineralization is found mainly in quartz veins in and associated with the aplitic porphyry. Molybdenum is the main economic sulphide accompanied by chalcopyrite and pyrite in lesser amounts. A sulphide mineralized, fracture controlled zone occurs along Whiting Creek (the Creek Zone). Chalcopyrite, pyrite, and minor bornite occur in potassic alteration in the granodiorite phase intrusive. A large zone of pyritized volcanics (the Creek Zone) lies in the south portion of the property. Only minor copper mineralization has been noted and no molybdenum mineralization has been observed.

AUTHOR'S QUALIFICATIONS

I, Richard D. Somerville, residing at #1704 2016 Fullerton Avenue, North Vancouver, British Columbia, V7P 1E6, certify that:

1.   I am a practising Consulting Geologist with offices at 240 -171 West Esplanade, North Vancouver, B.C., V7M 3K9.

2.   I am President of R. Somerville Geological and Mining Engineering Ltd.

3.   I am a Registered Professional Engineer of the Provinces of Ontario and British Columbia.

4.   I am a Fellow of the Geological Association of Canada and a Member of the Canadian Institute of Mining and Metallurgy.

5.   I am a graduate of Queen's University at Kingston, Ontario, having received a B.Sc. (honours) degree majoring in Geology, and a B.A. degree majoring in Physics and Mathematics.

6.   During the airborne geophysical program I was consulted professionally on a regular basis. During this period I visited the property, and I am satisfied that the work covered in this report was conducted in a proper and professional manner.

North Vancouver, British Columbia
January 15, 1994

R. Somerville, P. Eng.

BIBLIOGRAPHY

Diakow, L.;Mihalynuk, M. (1987)
    Geology of the Whitesail Reach and Troitsa Lake Areas,
    93E/10W,11E O.F. 1987-4
Duffel, S. (1959).
    Whitesail Lake Map Area, B.C. G.S.C. Memoir #229.
Jackson, A.W. (1993).
    Huckleberry Mtn. Copper Deposit - East Zone, November 15,
    1993.
James, D.H. (1976).
    Huckleberry - C.I.M. Special Vol. 15
MacIntyre, D.G., (1985).
    Geology and Mineral Deposits of the Tahtsa Lake District, West
    central B.C. E.M.P.R. Bull. 75, 1985
Smit,Hans (1992)
    Diamond Drill Report on the Whit Claims

APPENDIX #1

AERODAT REPORT

REPORT

ON A COMBINED
HELICOPTER-BORNE MAGNETIC, ELECTROMAGNETIC
RADIOMETRIC AND VLF-EM SURVEY

TAHTSA LAKE PROPERTY
PROVINCE OF BRITISH COLUMBIA
NTS 93 E/11

FOR

NEW CANAMIN RESOURCES LIMITED
SUITE 620, 171 WEST ESPLANADE STREET
NORTH VANCOUVER, BRITISH COLUMBIA
V7M 3K9

BY

GEONEX AERODAT INC.
3883 NASHUA DRIVE
MISSISSAUGA, ONTARIO
L4V 1R3

PHONE: 416 - 671-2446

October 8, 1993

R. W. Woolham, P. Eng.
Consulting Geophysicist

J9355

TABLE OF CONTENTS

LIST OF MAPS

The survey area is presented in two sets of numbered maps, a South Sheet and a North Sheet, in the following format:

BLACK LINE MAPS: (Scale 1:10,000)

Map No.   **Description**

1.   BASE MAP; screened topographic base map plus survey area boundary, and UTM grid.

2.   COMPILATION / INTERPRETATION MAP; with base map, flight path map and EM anomaly symbols with interpretation .

3   TOTAL FIELD MAGNETIC CONTOURS; with base map, EM anomalies and flight lines.

4.   VERTICAL MAGNETIC GRADIENT CONTOURS; with base map, EM anomalies and flight lines.

5A.   APPARENT RESISTIVITY CONTOURS; apparent resistivity calculated for the coplanar 4,175 Hz data, with base map, EM anomalies and flight lines.

5B.   APPARENT RESISTIVITY CONTOURS; apparent resistivity calculated for the coaxial 4,600 Hz data, with base map, EM anomalies and flight lines.

6.   VLF-EM TOTAL FIELD CONTOURS; with base map, EM anomalies and flight lines.

7A.   URANIUM COUNT RADIOMETRIC CONTOURS; with base map and flight lines.

7B.   THORIUM COUNT RADIOMETRIC CONTOURS; with base map and flight lines.

7C.   POTASSIUM COUNT RADIOMETRIC CONTOURS; with base map and flight lines.

7D.   TOTAL COUNT RADIOMETRIC CONTOURS; with base map and flight lines.

COLOUR MAPS: (Scale 1:10,000)

MAGNETIC

1.   TOTAL FIELD MAGNETICS; with superimposed contours, flight lines and EM anomaly symbols.

2.   VERTICAL MAGNETIC GRADIENT; with superimposed contours, flight lines and EM anomaly symbols.

RESISTIVITY

3A.   APPARENT RESISTIVITY; calculated for the coplanar 4,175 Hz data with superimposed contours, flight lines and EM anomaly symbols.

3B.   APPARENT RESISTIVITY; calculated for the coaxial 4,600 Hz data with superimposed contours, flight lines and EM anomaly symbols.

ELECTROMAGNETIC

4.   VLF-EM TOTAL FIELD; with superimposed contours, flight lines, and EM anomaly symbols.

5A.   HEM OFFSET PROFILES; coplanar 800 Hz and coaxial 935 Hz data with flight lines and EM anomaly symbols.

5B.   HEM OFFSET PROFILES; coplanar 4,175 Hz and coaxial 4,600 Hz data with flight lines and EM anomaly symbols.

5C.   HEM OFFSET PROFILES; coplanar 32,000 Hz data with flight lines and EM anomaly symbols.

RADIOMETRIC

6A.   URANIUM COUNT with superimposed contours and flight lines.

6B.   THORIUM COUNT with superimposed contours and flight lines.

6C.   POTASSIUM COUNT with superimposed contours and flight lines.

6D.   TOTAL COUNT with superimposed contours and flight lines.

SHADOW DERIVATIVE AND TERNARY MAPS: (Scale 1:20.000)

1.   TOTAL FIELD MAGNETICS SHADOW MAP; one of more of
   (A) parallel to the flight lines
   (B) perpendicular to the flight lines
   (C) at 45° or 135° to the flight lines

2.   TERNARY MAP OF URANIUM, THORIUM AND POTASSIUM

REPORT ON A
COMBINED HELICOPTER-BORNE
MAGNETIC, ELECTROMAGNETIC
RADIOMETRIC AND VLF-EM SURVEY
TAHTASA LAKE PROPERTY
PROVINCE OF BRITISH COLUMBIA

1. INTRODUCTION

This report describes an airborne geophysical survey carried out on behalf of New Canamin Resources Limited by Geonex Aerodat Inc. under a contract dated June 11, 1993. Principal geophysical sensors included a five frequency electromagnetic system, a high sensitivity cesium vapour magnetometer, a radiometric system and a two frequency VLF-EM system. Ancillary equipment included a colour video tracking camera, a radar altimeter, a power line monitor and a base station magnetometer.

The survey covers two areas designated Area A, about 90 square km. and Area B, about 25 square km. located between Prince Rupert and Prince George about 120 km south of Smithers. Total survey coverage was approximately 575 line kilometres (453 km over Area A and 122 km over Area B). The flight line spacing was 200 m. The Geonex Aerodat Job Number is J9355.

This report describes the survey, the data processing, data presentation and interpretation of the geophysical results. Electromagnetic anomalies have been identified and appear on selected map products as EM anomaly symbols with interpreted source characteristics. Conductive areas of interest are indicated on an interpretation map with designation number or letter. Prominent structural features interpreted from the magnetic results are also indicated. Recommendations concerning areas with favourable geophysical characteristics are made with reference to this compilation/interpretation map.

2. SURVEY AREA

The survey area is located just east of Tahtsa Lake 120 km south of Smithers and 110 km southwest of Burns Lake. Topography is shown on the 1:50,000 scale NTS map sheets 93 E/11. Local relief is rugged to moderate in areas A and B respectively. Elevations range from 2,900 feet to over 7,000 feet above mean sea level (amsl) in area A and from 3,100 feet to 4,200 feet amsl in area B.

The survey area is shown in the attached index map which includes local topography and latitude - longitude coordinates. This index map also appears on all black line map products. The flight line direction is north-south. Line spacing is 200 metres.

1

INDEX MAP
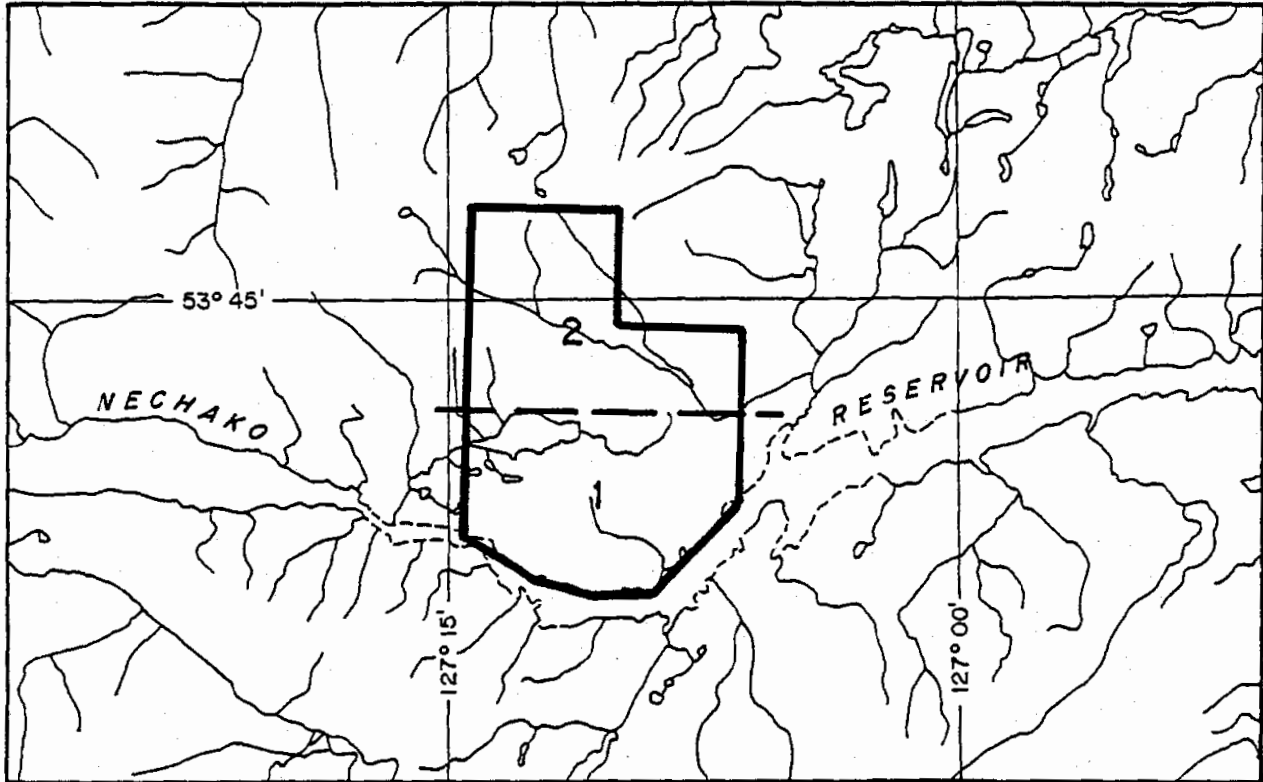
SURVEY AREA
TAHTSA LAKE PROPERTY
PROVINCE OF BRITISH COLUMBIA
NTS 93 E/11

3. SURVEY PROCEDURES

The survey was flown in the period from July 2 to 7, 1993. Principal personnel are listed in Appendix IV. A total of seven survey flights were required to complete the project.

The aircraft ground speed was maintained at approximately 60 knots (30 metres per second). The nominal EM sensor height was 30 metres (100 feet), consistent with the safety of the aircraft and crew.

Following equipment installation and testing, the ground based transponders of the radar ranging navigation system were installed at sites near the survey area. The base lines (or line between transponders) were flown to determine their separation. The results are used to check the UTM coordinates assigned to each transponder based on published NTS maps.

The UTM coordinates of survey area corners were taken from the published NTS maps. These coordinates are used to program the navigation system. A test flight was used to confirm that area coverage would be as required.

Thereafter the traverse lines are flown under the guidance of the navigation system. The operator also enters manual fiducials over prominent topographic features as seen on a topographic map. Survey lines which show excessive deviation were re-flown.

The magnetic tie lines were flown using visual navigation in areas of low topographic and magnetic relief. Aircraft position was taken from the navigation system.

Calibration lines are flown at the start, middle (if required) and end of every survey flight. These lines are flown outside of ground effects to record electromagnetic zero levels.

4. DELIVERABLES

The results of the survey are presented in a report plus maps. The report is presented in four copies. White print copies of all black line maps are folded and bound with the report. The colour maps are delivered in four copies. The shadow maps are delivered in two copies. The colour and shadow maps are rolled and delivered in map tube(s).

The black line maps show topography, UTM grid co-ordinates and the survey boundary. A full list of all map types is given at the beginning of this report. A summary is given following:

MAP NO.   DESCRIPTION

BLACK LINE

1   Base Map
2   Compilation/Interpretation Map
3   Total Field Magnetic Contours
4   Vertical Magnetic Gradient Contours
5A   Apparent Resistivity Contours - 4,175 Hz
5B   Apparent Resistivity Contours - 4,600 Hz
6   VLF-EM Total Field Contours
7A   Uranium Count Radiometric Contours
7B   Thorium Count Radiometric Contours
7C   Potassium Count Radiometric Contours
7D   Total Count Radiometric Contours

COLOUR

1   Total Field Magnetics
2   Vertical Magnetic Gradient
3A   Apparent Resistivity Contours - 4,175 Hz
3B   Apparent Resistivity Contours - 4,600 Hz
4   VLF-EM Total Field
5A   HEM Offset Profiles - 800 Hz and 935 Hz
5B   HEM Offset Profiles - 4,175 Hz and 4,600 Hz
5C   HEM Offset Profiles - 32,000 Hz
6A   Uranium Count Radiometric
6B   Thorium Count Radiometric
6C   Potassium Count Radiometric
6D   Total Count Radiometric
7   Total Field Magnetic Shadow
8   Radiometric Ternary

The processed digital data is organized on 9 track archive tape. Both the profile and the gridded data are saved on tape. A full description of the archive tape(s) is delivered with the tape(s).

All gridded data are also provided on diskettes suitable for displaying on IBM compatible 286 or 386 microcomputers using the Aerodat AXIS (Aerodat Extended Imaging System) or RTI (Real Time Imaging) software package.

All analog records, base station magnetometer records, flight path video tape and original map cronaflexes are delivered with the final presentation.

5. AIRCRAFT AND EQUIPMENT

5.1 Aircraft

A ASTAR helicopter, (C-FXHS), piloted by L. Stanley, owned and operated by Executive Helicopters Ltd, was used for the survey. L. Moore of Geonex Aerodat acted as navigator and equipment operator. Installation of the geophysical and ancillary equipment was carried out by Geonex Aerodat. The survey aircraft was flown at a mean terrain clearance of 60 metres (200 feet).

5.2 Electromagnetic System

The electromagnetic system was an Aerodat 5 frequency system. Two vertical coaxial coil pairs were operated at 935 Hz and 4,600 Hz and three horizontal coplanar coil pairs at 800 Hz 4,175 Hz and 32 kHz. The transmitter-receiver separation was 7 metres. Inphase and quadrature signals were measured simultaneously for the 6 frequencies with a time constant of 0.1 seconds. The HEM bird was towed 30 metres (100 feet) below the helicopter.

5.3 VLF-EM System

The VLF-EM System was a Herz Totem 2A. This instrument measures the total field and vertical quadrature components of two selected frequencies. The sensor was towed in a bird 10 metres below the helicopter.

VLF transmitters are designated "Line" and "Ortho". The line station is that which is in a direction from the survey area which is ideally normal to the flight line direction. This is the VLF station most often used because of optimal coupling with near vertical conductors running perpendicular to the flight line direction . The ortho station is ideally 90 degrees in azimuth away from the line station.

The transmitters used were:

NAA, Cutler, Maine broadcasting at 24.0 kHz. (line)
NSS, Annapolis, Maryland broadcasting at 21.4 kHz. (ortho)

5.4 Magnetometer

The magnetometer employed was a Scintrex H8 cesium, optically pumped magnetometer sensor. The sensitivity of this instrument is 0.001 nanoTesla at a 0.2 second sampling rate. The sensor was towed in a bird 15 metres (50 feet) below the helicopter (45 metres (150 feet) above the ground).

5.5 Gamma-Ray Spectrometer

An Exploranium GR-256 spectrometer coupled to 512 cubic inches of crystal sensor was used to record four channels of radiometric data. Spectrum stabilization is based on the 662 KeV peak from Cesium sources planted on the crystals.

The four channels recorded and their energy windows were as follows:

Channel	Window
Total Count (TC)	0.40 to 2.81 MeV
Potassium (K)	1.37 to 1.57 MeV
Uranium (U)	1.66 to 1.86 MeV
Thorium (Th)	2.41 to 2.81 MeV

The four channels of radiometric data were recorded at a 1 second update rate (counts per second - cps). Digital recording resolution is 1 cps.

5.6 Ancillary Systems

Base Station Magnetometer

An IFG-2 proton precession magnetometer was operated at the base of operations to record diurnal variations of the earth's magnetic field. The clock of the base station was synchronized with that of the airborne system to facilitate later correlation. Recording resolution was 1 nT. The update rate was 4 seconds.

External magnetic field variations were recorded on a 3" wide paper chart and in digital form. The analog record shows the magnetic field trace plotted on a grid. Each division of the grid (0.25") is equivalent to 1 minute (chart speed) or 5 nT (vertical sensitivity). The date, time and current total field magnetic value are printed every 10 minutes.

Radar Altimeter

A King KRA-10 radar altimeter was used to record terrain clearance. The output from the instrument is a linear function of altitude. The radar altimeter is checked after installation using a line marked off at intervals of 50 feet. A heavy weight is tied onto one end of the line. The helicopter moves up over the weight and the operator notes the radar altimeter reading at the 100, 150, 200 and 250 foot marks.

Tracking Camera

A Panasonic colour video camera was used to record flight path on VHS video tape. The camera was operated in continuous mode. The flight number, 24 hour clock time (to .01 second), and manual fiducial number are encoded on the video tape.

Radar Ranging Navigation System

A Motorola Miniranger Falcon 484 positioning system was used to guide the pilot over a programmed grid. The ranges to at least two ground stations were digitally recorded. The output sampling rate is 1 second. Ranges are recorded with a resolution of 0.1 m.

Analog Recorder

A RMS dot matrix recorder was used to display the data during the survey. Record contents are as follows:

Label	Contents	Scale
MAGF	Total Field Magnetics, Fine	2.5 nT/mm
MAGC	Total Field Magnetics, Course	25 nT/mm
VLT	VLF-EM, Total Field, Line Station	2.5% / mm
VLQ	VLF-EM, Vert. Quadrature, Line Station	2.5% / mm
VOT	VLF-EM, Total Field, Ortho Station	2.5% / mm
VOQ	VLF-EM, Vert. Quadrature, Ortho Station	2.5% / mm
CXI1	935 Hz, Coaxial, Inphase	2.5 ppm/mm
CXQ1	935 Hz, Coaxial, Quadrature	2.5 ppm/mm
CXI2	4,600 Hz, Coaxial, Inphase	2.5 ppm/mm
CXQ2	4,600 Hz, Coaxial, Quadrature	2.5 ppm/mm
CPI1	850 Hz, Coplanar, Inphase	5 ppm/mm
CPQ1	850 Hz, Coplanar, Quadrature	5 ppm/mm
CPI2	4,175 Hz, Coplanar, Inphase	10 ppm/mm
CPQ2	4,175 Hz, Coplanar, Quadrature	10 ppm/mm
CPI3	33,000 Hz, Coplanar, Inphase	20 ppm/mm
CPQ3	33,000 Hz, Coplanar, Quadrature	20 ppm/mm
TF	Radiometric - Total Field	10 counts/mm
K	Radiometric - Potassium	5 counts/mm
U	Radiometric - Uranium	2.5 counts/mm
T	Radiometric - Thorium	2.5 counts/mm
RALT	Radar Altimeter	10 ft/mm
PWRL	60 Hz Power Line Monitor	-

Data is recorded with positive - up, negative - down. This does not apply to the VLF data as seen on the analog records which is inverted.

The analog zero of the radar altimeter is 5 cm from the top of the analog record. A helicopter terrain clearance of 60 m (200 feet) should therefore be seen some 3 cm from the top of the analog record.

Chart speed is 2 mm/second. The 24 hour clock time is printed every 20 seconds. The total magnetic field value is printed every 30 seconds. The ranges from the radar navigation system are printed every minute.

Vertical lines crossing the record are operator activated manual fiducial markers. The start of any survey line is identified by two closely spaced manual fiducials. The end of any survey line is identified by three closely spaced manual fiducials. Manual fiducials are numbered in order. Every tenth manual fiducial is indicated by its number, printed at the bottom of the record.

Calibration sequences are located at the start and end of each flight and at intermediate times where needed.

Digital Recorder

A DGR-33 data system recorded the digital survey data on magnetic media. Contents and update rates were as follows:

DATA TYPE	RECORDING INTERVAL	RECORDING RESOLUTION
Magnetometer	0.2 s	0.001 nT
VLF-EM (4 Channels)	0.2 s	0.03%
HEM (8 Channels)	0.1 s	
coaxial		0.03 ppm
coplanar-800 Hz/4,175 Hz		0.06 ppm
coplanar -32 kHz		0.125 ppm
Radiometric	0.2 s	1 cps
Position (2 Channels)	0.2 s	0.1 m
Altimeter	0.2 s	0.05 m
Power Line Monitor	0.2 s	-
Manual Fiducial		
Clock Time		

8

6. DATA PROCESSING AND PRESENTATION

6.1 Base Map

The base map is taken from a photographic enlargement of the NTS topographic maps. A UTM reference grid (grid lines usually every kilometre) and the survey area boundary were added. After registration of the flight path to the topographic base map, topographic detail and the survey boundary are digitized. This digital image of the base map is used as the base for the colour and shadow maps.

6.2 Flight Path Map

Radar Ranging Navigation System

The digital flight path record consists of ranges to ground transponders and/or UTM coordinates. For the latter, UTM coordinates of the ground transponders are needed. Without better sources, these coordinates are taken off NTS topographic maps. Errors of several hundred meters are possible, particularly where the transponder is in an unmarked area. Flying the base line (to determine the true distance between transponders) and checking registration using manual fiducials/video tape will reduce these errors to acceptable limits. The UTM co-ordinates can also be checked using GPS.

Flight Path

The flight path is drawn using linear interpolation between x,y positions from the navigation system. These positions are updated every second (or about 3.0 mm at a scale of 1:10,000). These positions are expressed as UTM eastings (x) and UTM northings (y).

Occasional dropouts occur when ranges to the ground transponders are lost. Interpolation is used to cover short flight path gaps. The navigator's flight path and/or the flight path recovered from the video tape may be stitched in to cover larger gaps. Such gaps may be recognized by the distinct straight line character of the flight path.

The manual fiducials are shown as a small circle and labelled by fiducial number. The 24 hour clock time is shown as a small square, plotted every 30 seconds. Small tick marks are plotted every 2 seconds. Larger tick marks are plotted every 10 seconds. The line and flight numbers are given at the start and end of each survey line.

The flight path map is merged with the base map by matching UTM coordinates from the base maps and the flight path record. The match is confirmed by checking the position of prominent topographic features as recorded by manual fiducial marks or as seen on the flight path video record.

9

6.3   Electromagnetic Survey Data

The electromagnetic data were recorded digitally at a sample rate of 10 per second with a time constant of 0.1 seconds. A two stage digital filtering process was carried out to reject major sferic events and to reduce system noise.

Local sferic activity can produce sharp, large amplitude events that cannot be removed by conventional filtering procedures. Smoothing or stacking will reduce their amplitude but leave a broader residual response that can be confused with geological phenomena. To avoid this possibility, a computer algorithm searches out and rejects the major sferic events. The signal to noise ratio was further enhanced by the application of a low pass digital filter. This filter has zero phase shift which prevents any lag or peak displacement from occurring, and it suppresses only variations with a wavelength less than about 0.25 seconds. This low effective time constant gives minimal profile distortion.

Following the filtering process, a base level correction was made using EM zero levels determined during high altitude calibration sequences. The correction applied is a linear function of time that ensures the corrected amplitude of the various inphase and quadrature components is zero when no conductive or permeable source is present. The filtered and levelled data were used in the determination of apparent resistivity (see below).

6.4   Total Field Magnetics

The aeromagnetic data were corrected for diurnal variations by adjustment with the recorded base station magnetic values. No corrections for regional variations were applied. The corrected profile data were interpolated on to a regular grid using an Akima spline technique. The grid provided the basis for threading the presented contours. The minimum contour interval is 5 nT. A grid cell size of 25 m was used.

6.5   Vertical Magnetic Gradient

The vertical magnetic gradient was calculated from the gridded total field magnetic data. The calculation is based on a 17 x 17 point convolution in the space domain. The results are contoured using a minimum contour interval of 0.05 nT/m. Grid cell sizes are the same as those used in processing the total field data.

6.6   Apparent Resistivity

The apparent resistivity is calculated by assuming a 200 metre thick conductive layer over resistive bedrock. The computer determines the resistivity that would be consistent with the sensor elevation and recorded inphase and quadrature response amplitudes at the selected frequency. The apparent resistivity profile data was re-interpolated onto a regular

grid at a 25 metres true scale interval using an Akima spline technique and contoured using logarithmically arranged contour intervals. The minimum contour interval is 0.1 log(ohm.m).

The highest measurable resistivity is approximately equal to the transmitter frequency. The lower limit on apparent resistivity is rarely reached.

6.7   VLF-EM

The VLF Total Field data from the Line Station is levelled such that a response of less than 0% is seen in non-anomalous regions. The corrected profile data are interpolated onto a regular grid using an Akima spline technique. The grid provided the basis for threading the presented contours. The minimum contour interval is 1%. Grid cell size is 25 m.

6.8   Radiometric Data

The four channels of radiometric data are subject to a four stage data correction process.

The stages are
- low pass filter (seven point Hanning)
- background removal
- terrain clearance correction
- compton stripping correction

The Compton stripping factors used were

alpha	0.271	(Th into U)
beta	0.405	(Th into K)
gamma	0.676	(U into K)
a	0.05	(U into Th)
b	-0.01	(K into Th)
g	0.001	(K into U)

where alpha, beta and gamma are the forward stripping coefficients and a, b, g are the backward stripping coefficients. These coefficients are taken in part from the sample checks done at the start of each flight.

The altitude attenuation coefficients used were 0.0072 (TC), 0.0085 (K), 0.0082 (U) and 0.0067 (Th). The units are metres $^{-1}$. These coefficients are taken from GSC publications for similar radiometric systems. Radiometric data were corrected to a mean terrain clearance of 60 m.

The corrected data were interpolated on a square grid (cell size 25 m) using an Akima spline technique. The grids provided the basis for threading the presented contours. The minimum contour intervals are *__ cps (TC), *_ cps (K), *_ cps (U) and *___ cps (Th).

7. INTERPRETATION

7.1 Area Geology

The geology consists of Middle Jurassic, Hazelton Group rocks made up of intermediate to mafic volcanics, argillite and arenaceous rocks. Strike and dips of the rocks is quite variable. Dips are generally between 10 and 60 degrees. Lead, zinc, silver and gold occurrences are known in the area.

7.2 Magnetic Interpretation

The total field magnetic responses reflect major changes in the magnetite content of the underlying rock units. The amplitude of the magnetic responses relative to the regional background help to assist in identifying specific magnetic and non-magnetic units related to, for example, mafic flows or tuffs, mafic to ultramafic intrusives, felsic intrusives, felsic volcanics and/or sediments etc. Obviously, several geological sources can produce the same magnetic response. These ambiguities can be reduced considerably if basic geological information on the area is available to the geophysical interpreter.

In addition to amplitude variations, magnetic patterns related to the geometry of the particular rock unit also help in determining the probable source of the magnetic response. For instance, long narrow magnetic linears usually reflect mafic tuff or flow horizons while semi-circular features with complex magnetic amplitudes may be produced by local plug-like intrusive sources such as pegmatites, carbonatites or kimberlites.

The calculated vertical magnetic gradient assists considerably in mapping weaker magnetic linears that are partially masked by nearby higher amplitude magnetic features. The broad zones of higher magnetic amplitude, however, are severely attenuated in the vertical magnetic gradient results. These higher amplitude zones reflect rock units having magnetic susceptibility signatures. For this reason both the total and gradient magnetic data sets must be evaluated.

Theoretically the zero contour of the magnetic gradient map marks the contacts or limits of large magnetic sources. This applies to wide sources, greater than 50 metres, having simple slab geometries and shallow depth.(See discussion in Appendix I) Thus the gradient map also aids in the more accurate delineation of contacts between differing magnetic rock units.

12

The cross cutting structures shown on the interpretation map are based on interruptions and discontinuities in the magnetic trends. Generally, sharp folding of magnetic units will produce a magnetic pattern indistinguishable from a fault break. Thus these structures have been designated as fold/fault features.

7.3   Magnetic Survey Results and Conclusions

To facilitate the following discussion of the magnetic results it is suggested that the interpretation map be compared with the total field and vertical gradient magnetic colour contour maps either as overlays or side by side.

Area A

The magnetic background is interpreted to be approximately 57,000 nanoTesla (nT). Amplitudes range from about 3,800 nT above background to 400 nT below background. Magnetic amplitudes of 1,000 to 2,000 nT above background indicate a higher than usual magnetite content of the underlying rocks. Usually intermediate to mafic volcanics tend to have amplitudes of 500 to 1,000 nt above background. Thus the high magnetic amplitudes in this survey area suggest ultramafic rocks as extrusives or intrusives may be present, or iron formation. Regional geological information indicates, however, only gabbros or basalts are present. It is probable that basalt flow rocks have a high magnetite content in this area.

Major fold/fault structures have been interpreted from the discontinuities and interruptions in the magnetic trends. Some of these features may actually relate to contact horizons rather than faults. Detailed geological information will help to resolve and confirm the source of these structures.

The higher amplitude anomalous areas, approximately 700 nT above background or higher, are designated on the map as magnetic complexes. Their boundaries are interpreted from the vertical gradient zero contour line. In some locations the asymmetry of the flanks of the large anomalies gives a qualitative indication of the dip or plunge of the magnetic body. These dip directions are indicated with a large arrow.

Lower amplitude intermediate positive magnetic responses are shown as linear solid lines or, if very weak, as dashed lines. Some of the intermediate amplitude anomalies may be related to wide bodies rather than narrow sheet sources implied by the line designation. The variation in magnetic amplitude relates to the thickness of the source rock as well as the magnetite content. Shallow dipping magnetic bodies will also produce broad total field anomalies. These anomalies are resolved into narrower features on the vertical gradient map. There are several low amplitude below background zones, designated on the interpretation map, that probably reflect felsic volcanic rocks, felsic intrusives or sediments. Local alteration effects sometimes produce anomalous below background areas.

13

The wide very high amplitude areas form two complex magnetic cores. One is centred on the south sheet the other covers most of the north sheet. The complex on the north sheet forms a concentric sinuous ring around a central below background core. The dip directions interpreted from the magnetics suggest that this magnetic complex may reflect an antiform with a northwest to north striking fold axis as shown on the interpretation map. The structure probably consists of felsic or sedimentary rocks in the centre surrounded by mafic volcanics. Secondary smaller fold centres are suggested by the semi-circular patterns on the west side of the complex.

The magnetic complex on the south sheet is more erratic. Nonetheless, the anomaly patterns suggest there are local fold axes present, as shown on the interpretation map, which probably relate to synform and/or antiform structures. Note that the most southerly east-west striking high amplitude anomaly has the highest magnetic response of the whole area. It is coincident with a local topographic high.

Area B

The magnetic background is interpreted to be approximately 57,050 nanoTesla (nT). Amplitudes range from about 550 nT above background to 250 nT below background. These amplitudes are much lower than those seen in area A. The anomaly patterns form high amplitude magnetic complexes producing a "U" shaped structure with superimposed east-west trends. Mafic volcanics or intrusives may be the source of these responses. The complex encloses local below background negative magnetic areas as shown on the interpretation map. As suggested previously, these low amplitude areas probably relate to felsic or sedimentary rocks but may also indicate local areas of alteration. A local ring structure is present in the north central part of the survey block flanking the east side of the west arm of the U structure. This feature is coincident with a local topographic high and may be worth investigation.

7.4   Electromagnetic Anomaly Selection/Interpretation

Usually two sets of stacked colour coded profile maps of one coaxial and one coplanar inphase and quadrature responses are used to select conductive anomalies of interest. Selection of anomalies is based on conductivity as indicated by the inphase to quadrature ratios of the 935 Hz and 4,600 Hz data, anomaly shape, and anomaly profile characteristics relative to coaxial and corresponding coplanar responses.(see discussion and figure in Appendix I)

It is difficult to differentiate between responses associated with the edge effects of flat lying conductors and actual poor conductivity bedrock conductors on the edge of or overlain by flat lying conductors. Poor conductivity bedrock conductors having low dips will also exhibit responses that may be interpreted as surficial overburden conductors. In such cases, where the source of the conductive response appears to be ambiguous, the anomaly is still selected for plotting. In some situations the conductive response has line

14

to line continuity and some magnetic association thus providing possible evidence that the response is related to an actual bedrock source.

The calculation of the depth to the conductive source and its conductivity is based on the 4,600 Hz data using a thin vertical sheet model. The amplitude of the inphase and quadrature responses are used for the calculations which are automatically determined by computer. These data are listed in Appendix II and the depth and conductivity values are shown with each plotted anomaly. Further detailed discussion and illustration of the determination of these values is contained in Appendix I.

The selected anomalies are automatically categorized according to their conductivity and amplitude. The calculation of the conductivity of low amplitude anomalies can be very inaccurate. Therefore, anomalies having amplitudes below a certain level and/or low conductivity value are given a zero rating with the category increasing for increasing conductivity values that are statistically reliable.

7.5   VLF Electromagnetic Survey

This high frequency type of survey, utilizing fixed government communication transmitter stations, tends to detect long strike length and/or surficial poor conductivity sources such as swamps, creeks and rivers. Conductors that are optimum coupled with the primary field will usually predominate over those with other strike directions. In some instances anomalies will be produced by variations in topographic relief.

This appears to be the case for Area A where many of the VLF anomalies are associated with the flanks of topographic highs or swampy areas. There is a regional east-west grain to the strike directions of the VLF conductive trends which doesn't correlate with the magnetic trend directions. This suggests that most of the VLF responses are probably not related to bedrock sources. In addition there is poor correlation between the conductive responses detected by the helicopter electromagnetic system and those detected by the VLF survey.

In Area B the VLF station ceased operation and no data are available for this area.

7.6   Electromagnetic Survey Results and Conclusions

Area A

Conductive flat lying material is contributing to the electromagnetic responses in various degrees throughout the survey block. These areas are characterized by identically shaped coaxial and coplanar response profiles. This is a typical response shape usually seen over a flat lying conductor as illustrated in Appendix I, in the figure entitled "HEM Response Profile Shapes ....." profile I. These areas of apparent flat lying conductive sources have

15

not been indicated on the interpretation map or anomaly map but show up on the apparent resistivity maps as broad low resistivity zones.

Most of the electromagnetic anomalies selected for plotting have poor conductivity and appear to be related to flat lying or shallow dipping sources. In many areas the profile response was broad and individual peaks were difficult to select with confidence. These broad conductive areas are designated on the anomaly maps but usually contain individual peak picks. It is difficult to determine if conductive overburden is producing the effects or shallow dipping conductive bedrock sources. Where conductors are coincident with lakes, swamps or drainage areas they can usually be considered as surficial conductive responses. This occurs in a few areas but many areas of conductivity fall on ridges, topographic highs or their flanks suggesting a bedrock source is producing the conductive responses.

The high magnetite content of the rocks has produced many negative in-phase susceptibility responses. If there is no positive quadrature response associated with these anomalies magnetite is probably the only source present. If a positive quadrature response is present, however, then a conductive source such as pyrite or pyrrhotite may be contributing to the anomaly. These types of anomalies are designated separately on the EM anomaly map. In many areas they occur within the larger zones of poor conductivity response.

Where there is line to line continuity of peaks or zones of conductivity they have been grouped together as shown on the interpretation map. The resistivity maps have been used as an aid to mark the boundaries of some of the more complex zones. The source of these anomalies is interpreted to be largely conductive sediments containing graphite and/or pyrite/pyrrhotite. Nevertheless, specific conductive areas of possible interest and recommended for further investigation are designated on the interpretation map. These anomalous areas have been numbered from north to south in Area A and west to east in Area B.

Area A

Anomalies 1, 2, 3, 4, and 6 fall within larger conductive zones in the north part of the north sheet. All of these conductors have strong negative in-phase responses. Conductive areas 3 and 4 are within low amplitude below background magnetic areas and area 4 covers an interpreted cross-cutting fault structure. Anomalies 5, 7, 8 and 9 on the north sheet are local conductive/magnetic zones on the rim of the regional circular magnetic feature described previously.

On the south sheet, there are two conductive areas designated for further investigation. Conductors 10A/10B and 11A/11B straddle interpreted fault structures. Conductors 10A and 10B have a magnetic component. Other conductive complexes on this sheet cover drainage areas, swampy low lying areas or lakes and may be related to conductive surficial material.

Area B

There are very few conductive intercepts in this area that can be attributed to bedrock sources. Those selected for plotting have poor conductivity and very few anomaly clusters form any conductive pattern. Nonetheless, four conductive areas have been designated for possible investigation on a low priority basis. Conductors 1 and 2 on the west side of the survey block are related to an interpreted fault zone. Conductors 3 and 4 also have an association with a major east-west interpreted fault structure and conductor 4 is in a low amplitude magnetic area.

7.7   Radiometric Interpretation

The ability to detect natural occurring radiation, whether on the ground or from an airborne platform, depends on a number of factors listed as follows:

Count Time

Measurements or count rate statistics are more reliable the longer the detector is in position over a particular location. Therefore in airborne surveying, traverse speed is an important factor in detecting radiation sources. For this reason STOL aircraft and helicopters are a favoured platform for radiometric surveys.

Detector size

The detector crystal volume and thickness determine the sensitivity of the radiometric system to radiation. For accurate measurement and differentiation of higher energy levels of radiation, a large crystal volume is a pre-requisite.

Distance from Source (Altitude)

The attenuation or absorption of radiation in air, although not a significant factor in ground surveys, is a factor in airborne surveys. Normalization of the radiation amplitude data for altitude variations of the aircraft during the survey is necessary. The attenuation is not significant for large areal sources of radiation but is quite severe for localized point sources.

17

Overburden Cover

Radiation can be completely masked by one foot of rock or three feet of unconsolidated overburden.

Source Geometry

A large exposed outcrop of slightly radioactive material, such as granite which usually has a high potassium count, will be easily detectable from the air. A small outcrop of highly radioactive material, containing an appreciable amount of pitchblende for instance, may not be detectable unless the sensor passes directly over the outcrop and/or is quite close to it.

Source Characteristics

The type and percentage concentration of radioactive minerals present in the rock will determine radiation amplitudes and therefore the ability of the sensor to measure the radiation.

The above factors must be taken into consideration when evaluating and interpreting radiometric surveys. Variations in radiation amplitudes may only be a factor of overburden cover. As a result, an outcrop map of the survey area is very useful for initial evaluation of radioactive element concentrations.

Shales and felsic intrusives tend to have high potassium and thorium levels. Mafic intrusives, sandstone and especially limestone have concentrations of one half to one tenth of the highest levels. Specific intrusives types, such as pegmatites, can have levels of potassium, uranium and thorium, in the order of three to four times the amounts normally present. Uranium ore can contain concentrations of radioactive minerals one to four orders of magnitude greater than normally encountered.

Thus, interpretation of the source of radioactive anomalies, even when the uranium, thorium and potassium thresholds are separated, can be difficult and ambiguous. In some geological environments, specific rock units have higher or lower uranium/thorium, uranium/potassium, or thorium/potassium ratios. Additional diagnostic information is sometimes available when such ratio maps are generated and compared to known geological parameters.

For this interpretation, amplitude characteristics for the various channels will be discussed relative to the features mapped by the magnetic and electromagnetic results.

18

7.8   Radiometric Survey Results and Conclusions

Area A

With the exception of the extreme north portion of this area, the radiometric responses are at background levels. Local, slightly anomalous areas are usually only 1 1/2 times background and may reflect local outcrop exposures.

In the north part of the sheet there is an erratic, highly anomalous area from 5 to 10 times background in amplitude. This anomalous zone registers on all three potassium, thorium and uranium channels. It has a spatial relationship to both the conductive and, in part, magnetic anomalies indicated on the interpretation map. Shales often have high potassium and thorium levels and this may be the source of the radiometric responses.

The designated conductive areas 1, 2, 3, 4 and 6 cover the higher amplitude radiometric responses. Investigation of the source of these radiometric anomalies can be completed at the same time as the conductive areas are evaluated.

Area B

Most of the anomalies in this block are about 1 1/2 times background. There are a few local, higher amplitude anomalies but they do not appear to have any relationship to the other geophysical signatures and may be local outcrop exposures.

8.   RECOMMENDATIONS

Local geological information or the ore target model for the survey area was not made available to the author. As a result, selection of geophysical anomalies for further investigation is based on the structural and magnetic associations of the designated conductors as well as their relative conductivity. The recommendations to follow should be evaluated in conjunction with known geological and geochemical information, if available. Usually, some level of priority is assigned to the designated anomalies. In this survey, however, there is no specific geophysical response that can be considered more favourable than any other.

Area A
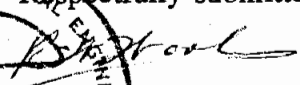
The below background low amplitude magnetic areas in this survey block should be explained. Most of the areas are probably related to sediments or felsic rocks however some of the more intense localized negative areas are recommended for further investigation. Such areas are located around conductor 3 and possibly south of conductor 5 on the north sheet and the low amplitude area in the extreme southwest portion of the south sheet.

All of the designated conductors on the north and south sheets are recommended for evaluation. This work will also aid in confirming some of the fold and fault structures interpreted from the geophysical data.

The high amplitude radiometric responses in the north part of the north sheet warrant investigation. This work can be done in conjunction with the evaluation of conductive areas 1, 2, 3, 4 and 6.

Area B

There are four conductive zones designated on this map that are suggested for further evaluation on a low priority basis. They have a spatial association with a fault zone. In addition, the magnetic ring structure just to the northwest of conductor 3, designated A, deserves investigation as well as the below background magnetic area B in the southwest corner of the map sheet.

Respectfully submitted,

R. W. Woolham, P.Eng.
Consulting Geophysicist

for

GEONEX AERODAT INC.

J9355

October 8, 1993

20
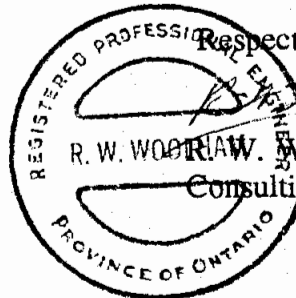
APPENDIX I

GENERAL INTERPRETIVE CONSIDERATIONS

GENERAL INTERPRETIVE CONSIDERATIONS

Electromagnetic

The Aerodat six frequency system utilized two different transmitter-receiver coil geometries. The traditional coaxial coil configuration is operated at three widely separated frequencies. The horizontal coplanar coil configuration is similarly operated at three different frequencies where at least one pair is approximately aligned with one of the coaxial frequencies.

The electromagnetic response measured by the helicopter system is a function of the "electrical" and "geometrical" properties of the conductor. The "electrical" property of a conductor is determined largely by its electrical conductivity, magnetic susceptibility and its size and shape; the "geometrical" property of the response is largely a function of the conductor's shape and orientation with respect to the measuring transmitter and receiver.

Electrical Considerations

For a given conductive body the measure of its conductivity or conductance is closely related to the measured phase shift between the received and transmitted electromagnetic field. A small phase shift indicates a relatively high conductance, a large phase shift lower conductance. A small phase shift results in a large inphase to quadrature ratio and a large phase shift a low ratio. This relationship is shown quantitatively for non-magnetic vertical half-plane and half-space models on the accompanying phasor diagrams. Other physical models will show the same trend but different quantitative relationships.

The phasor diagram for the vertical half-plane model, as presented, is for the coaxial coil configuration with the amplitudes in parts per million (ppm) of the primary field as measured at the response peak over the conductor. To assist the interpretation of the survey results the computer is used to identify the apparent conductance and depth of selected anomalies. The results of this calculation are presented in anomaly listings included in the survey report and the conductance and inphase amplitude are presented in symbolized form on the map presentation.

The conductance estimate is most reliable when anomaly amplitudes are large and background resistivities are high. Where the EM anomaly is of low amplitude and background resistivities are low, the conductance estimates are much less reliable. In such situations, the conductance estimate is often quite low regardless of the true nature of the conductor. This is due to the elevated background response levels in the quadrature channel. In an extreme case, the conductance estimate should be discounted and should not prejudice target selection.

The conductance and depth values as presented are correct only as far as the model approximates the real geological situation. The actual geological source may be of limited length, have significant dip, may be strongly magnetic. Its conductivity and thickness may vary with depth

AERODAT HEM SYSTEM RESPONSE
HOMOGENEOUS HALF-SPACE
(UNIFORM EARTH)

HORIZONTAL COPLANAR COILS

AERODAT HEM SYSTEM RESPONSE
HOMOGENEOUS HALF-SPACE
(UNIFORM EARTH)

VERTICAL COAXIAL COILS

AERODAT HEM SYSTEM RESPONSE
VERTICAL HALF-PLANE

QUADRATURE (ppm)

IN-PHASE (ppm)

7.0 m

R

h

Surface

d

σt

f - Frequency (Hz)
σt - Conductance (siemens)
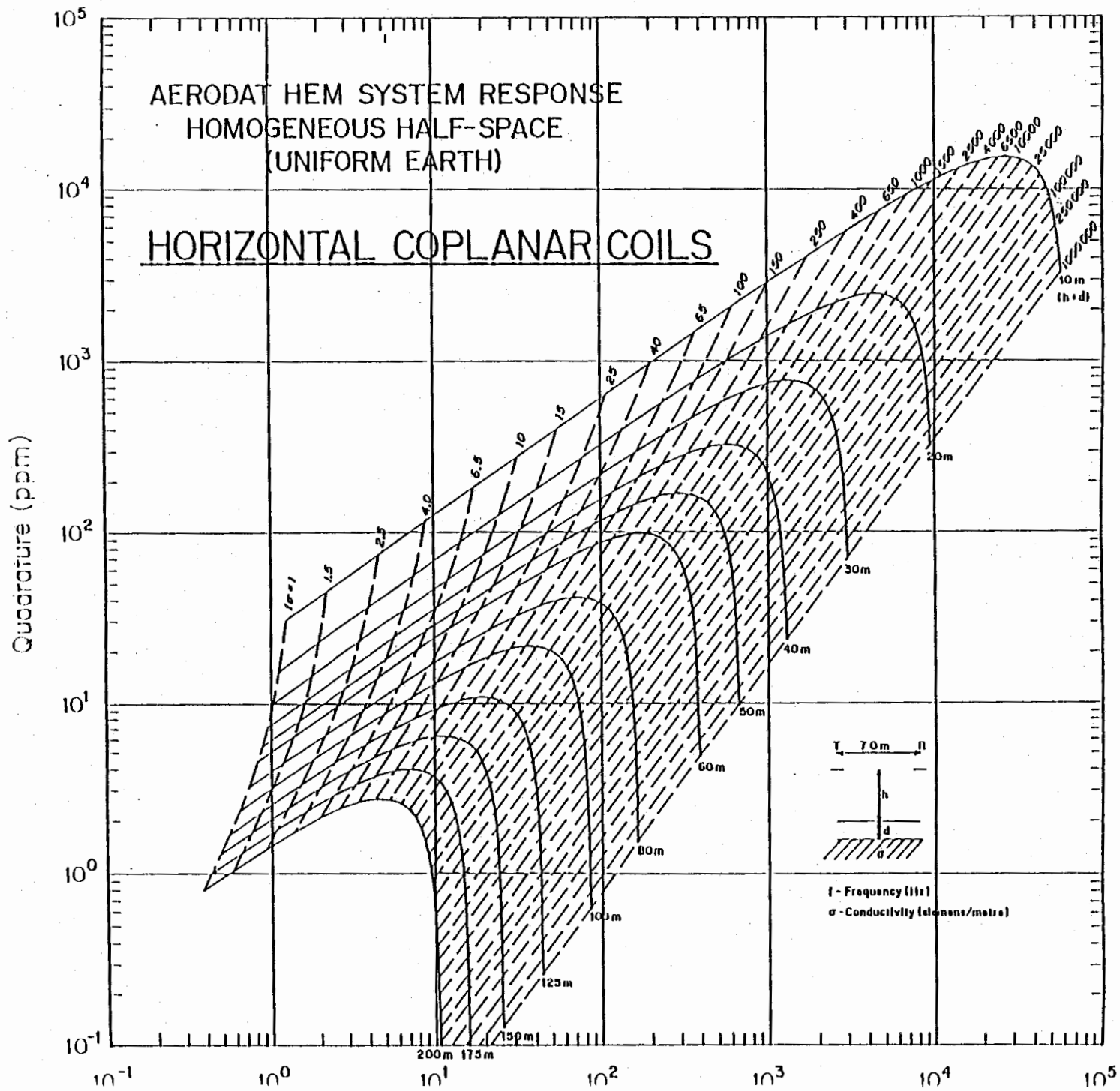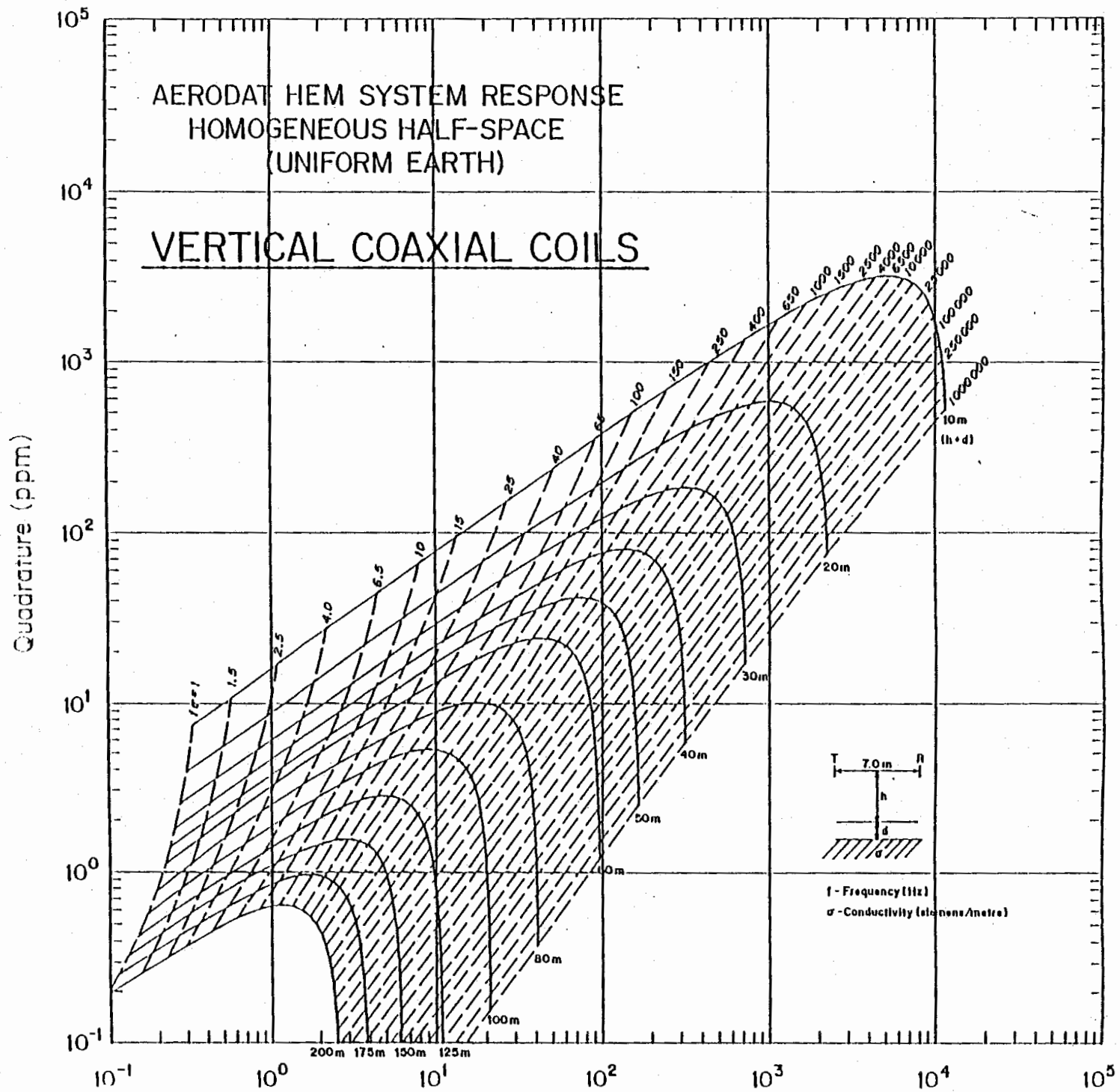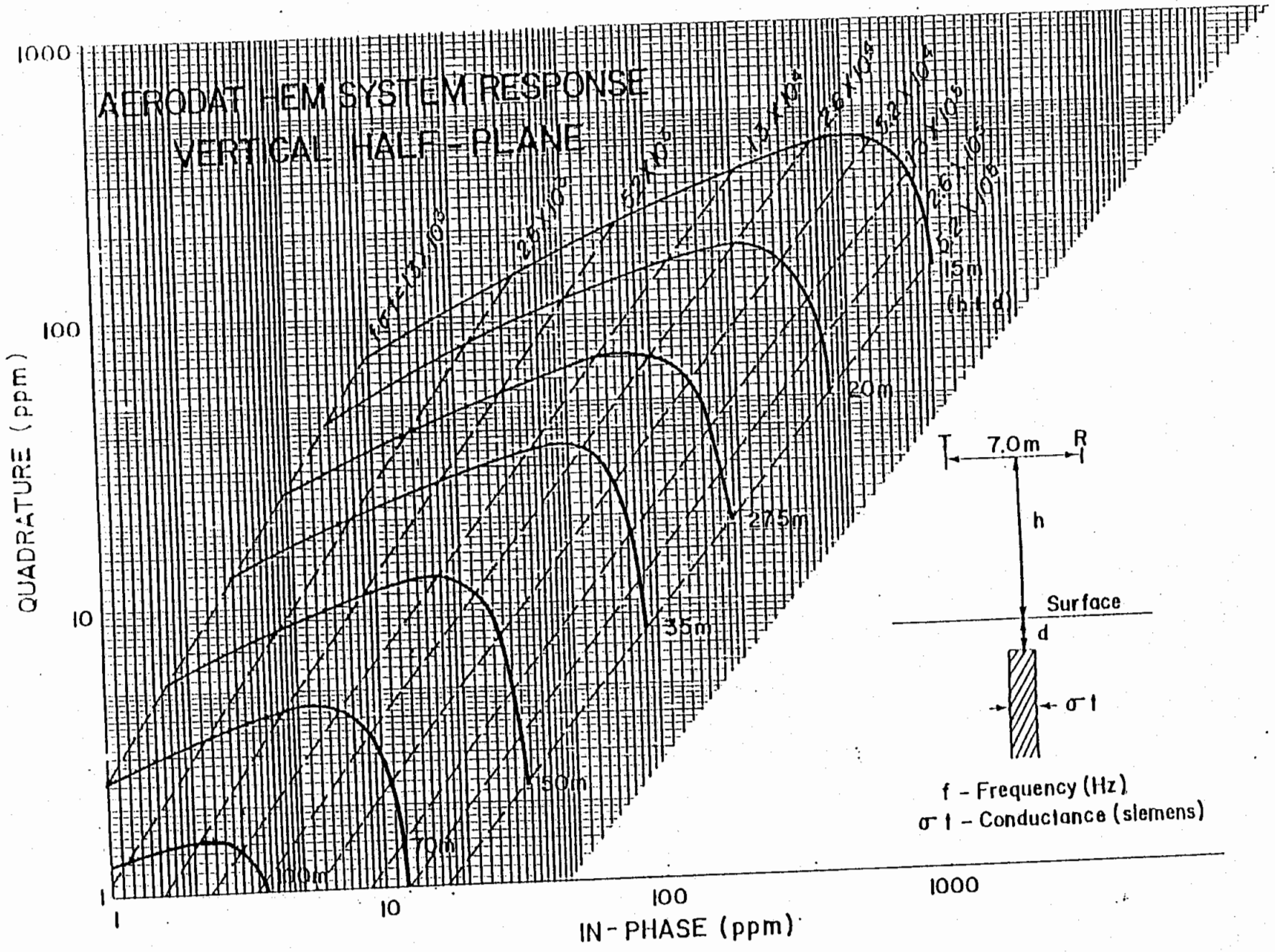
and/or strike and adjacent bodies and overburden may have modified the response. In general the conductance estimate is less affected by these limitations than is the depth estimate, but both should be considered as relative rather than absolute guides to the anomaly's properties.

Conductance in mhos is the reciprocal of resistance in ohms and in the case of narrow slab-like bodies is the product of electrical conductivity and thickness.

The higher ranges of conductance, greater than 2-4 mhos, indicate that a significant fraction of the electrical conduction is electronic rather than electrolytic in nature. Materials that conduct electronically are limited to certain metallic sulphides and to graphite. High conductance anomalies, roughly 10 mhos or greater, are generally limited to massive sulphides or graphites.

Sulphide minerals, with the exception of such ore minerals as sphalerite, cinnabar and stibnite, are good conductors. Sulphides may occur in a disseminated manner that inhibits electrical conduction through the rock mass. In this case the apparent conductance can seriously underrate the quality of the conductor in geological terms. In a similar sense the relatively non-conducting sulphide minerals noted above may be present in significant concentrations in association with minor conductive sulphides, and the electromagnetic response will only relate to the minor associated mineralization. Indicated conductance is also of little direct significance for the identification of gold mineralization. Although gold is highly conductive, it would not be expected to exist in sufficient quantity to create a recognizable anomaly. Minor accessory sulphide mineralization may however provide a useful indirect indication.

In summary, the estimated conductance of a conductor can provide a relatively positive identification of significant sulphide or graphite mineralization. A moderate to low conductance value does not rule out the possibility of significant economic mineralization.

Geometrical Considerations

Geometrical information about the geologic conductor can often be interpreted from the profile shape of the anomaly. The change in shape is primarily related to the change in inductive coupling among the transmitter, the target, and the receiver. The accompanying figure shows a selection of HEM response profile shapes from nine idealized targets. Response profiles are labelled A through I. These labels are used in the discussion which follows.

In the case of a thin, steeply dipping, sheet-like conductor, the coaxial coil pair will yield a near symmetric peak over the conductor. On the other hand, the coplanar coil pair will pass through a null couple relationship and yield a minimum over the conductor, flanked by positive side lobes.(Profile A) As the dip of the conductor decrease from vertical, the coaxial anomaly shape changes only slightly, but in the case of the coplanar coil pair the side lobe on the down dip side strengthens relative to that on the up dip side.(Profiles B and C).

As the thickness of the conductor increases, induced current flow across the thickness of the

HEM RESPONSE PROFILE SHAPE AS AN
INDICATOR OF CONDUCTOR GEOMETRY

COAXIAL   vertical scale 1 ppm/unit
COPLANAR vertical scale 4 ppm/unit
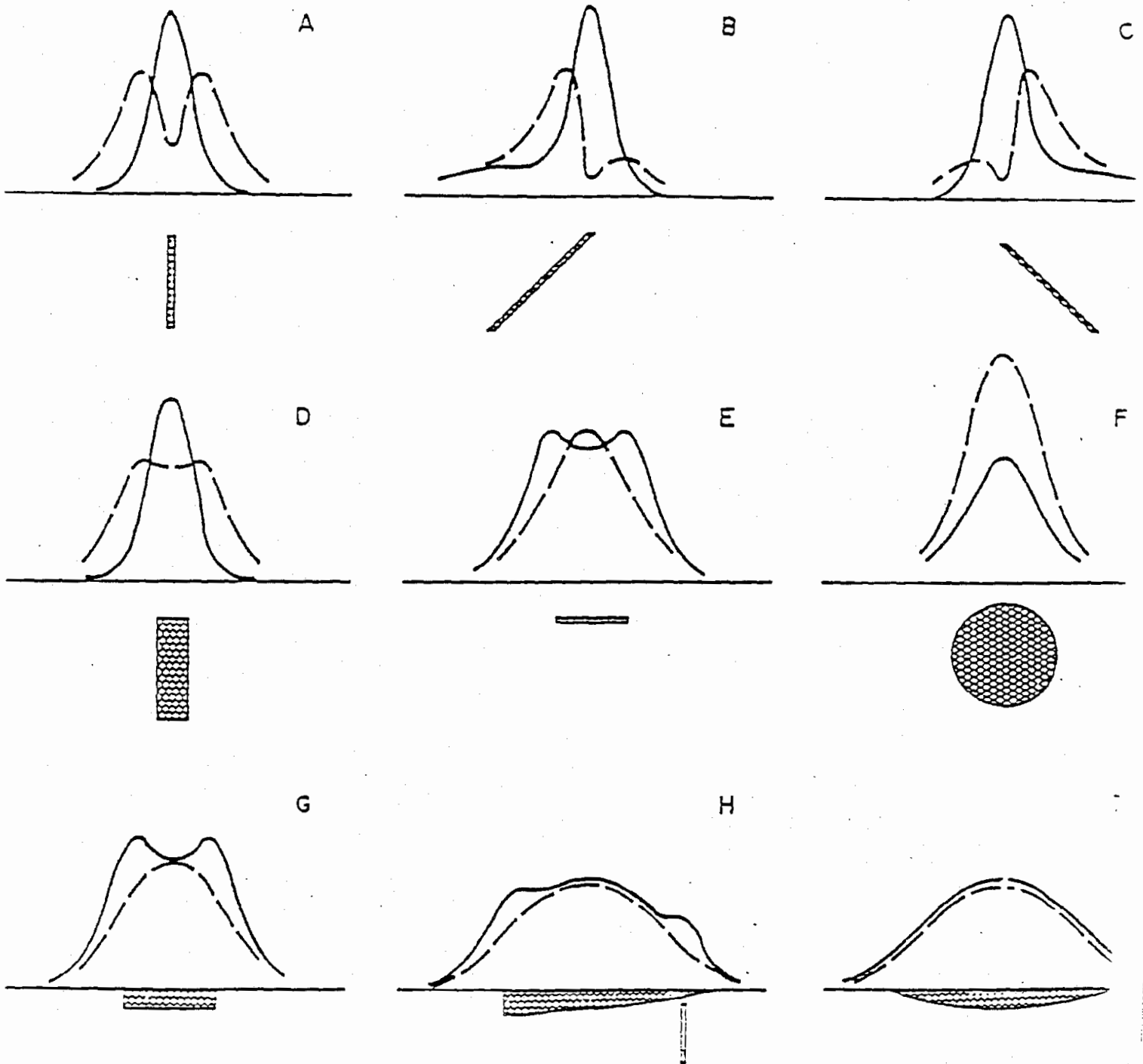
conductor becomes relatively significant and complete null coupling with the coplanar coils is no longer possible.(Profile D) As a result, the apparent minimum of the coplanar response over the conductor diminishes with increasing thickness, and in the limiting case of a fully 3 dimensional body or a horizontal layer or half-space, the minimum disappears completely.

A horizontal conducting layer such as a horizontal thin sheet or overburden will produce a response in the coaxial and coplanar coils that is a function of altitude (and conductivity if not uniform). The profile shape will be similar in both coil configurations with an amplitude ratio (coplanar:coaxial) of about 4:1*.(Profiles E and G).

In the case of a spherical conductor, the induced currents are confined to the volume of the sphere, but not relatively restricted to any arbitrary plane as in the case of a sheet-like form. The response of the coplanar coil pair directly over the sphere may be up to 8* times greater than that of the coaxial pair.(Profile F)

In summary, a steeply dipping, sheet-like conductor will display a decrease in the coplanar response coincident with the peak of the coaxial response. The relative strength of this coplanar null is related inversely to the thickness of the conductor. A pronounced null indicates a relatively thin conductor. The dip of such a conductor can be inferred from the relative amplitudes of the side-lobes.

Massive conductors that could be approximated by a conducting sphere will display a simple single peak profile form on both coaxial and coplanar coils, with a ratio between the coplanar to coaxial response amplitudes as high as 8*.

Overburden anomalies often produce broad poorly defined anomaly profiles.(Profile I) In most cases, the response of the coplanar coils closely follows that of the coaxial coils with a relative amplitude ratio of 4*.

Occasionally, if the edge of an overburden zone is sharply defined with some significant depth extent, an edge effect will occur in the coaxial coils. In the case of a horizontal conductive ring or ribbon, the coaxial response will consist of two peaks, one over each edge; whereas the coplanar coil will yield a single peak.(Profile H)

* It should be noted at this point that Aerodat's definition of the measured ppm unit is related to the primary field sensed in the receiving coil without normalization to the maximum coupled (coaxial configuration). If such normalization were applied to the Aerodat units, the amplitude of the coplanar coil pair would be halved.

Magnetics

The Total Field Magnetic Map shows contours of the total magnetic field, uncorrected for regional variation. Whether an EM anomaly with a magnetic correlation is more likely to be

caused by a sulphide deposit than one without depends on the type of mineralization. An apparent coincidence between an EM and a magnetic anomaly may be caused by a conductor which is also magnetic, or by a conductor which lies in close proximity to a magnetic body. The majority of conductors which are also magnetic are sulphides containing pyrrhotite and/or magnetite. Conductive and magnetic bodies in close association can be, and often are, graphite and magnetite. It is often very difficult to distinguish between these cases. If the conductor is also magnetic, it will usually produce an EM anomaly whose general pattern resembles that of the magnetics. Depending on the magnetic permeability of the conducting body, the amplitude of the inphase EM anomaly will be weakened, and if the conductivity is also weak, the inphase EM anomaly may even be reversed in sign.

The interpretation of contoured aeromagnetic data is a subject on its own involving an array of methods and attitudes. The interpretation of source characteristics for example from total field results is often based on some numerical modelling scheme. The vertical gradient data is more legible in some aspects however and useful inferences about source characteristics can often be read off the contoured VG map.

The zero contour lines in contoured VG data are often sited as a good approximation to the outline of the top of the magnetic source. This only applies to wide (relative to depth of burial) near vertical sources at high magnetic latitudes. It will give an incorrect interpretation in most other cases.

Theoretical profiles of total field and vertical gradient anomalies from tabular sources at a variety of magnetic inclinations are shown in the attached figure. Sources are 10, 50 and 200 m wide. The source-sensor separation is 50 m. The thin line is the total field profile. The thick line is the vertical gradient profile.

The following comments about source geometry apply to contoured vertical gradient data for magnetic inclinations of 70 to 80°.

Outline

Where the VG anomaly has a single sharp peak, the source may be a thin near-vertical tabular source. It may be represented as a magnetic axis or as a tabular source of measureable width - the choice is one of geological preference.

Where the VG anomaly has a broad, flat or inclined top, the source may be a thick tabular source. It may be represented as a thick body where the width is taken from the zero contour lines if the body dips to magnetic north. If the source appears to be dipping to the south (i.e. the VG anomaly is asymmetric), the zero contours are less reliable indicators of outline. The southern most zero contour line should be ignored and the outline taken from the northern zero contour line and the extent of the anomaly peak width.

INCLINATION OF
MAGNETIC FIELD

TOTAL FIELD

VERTICAL GRADIENT

$\frac{1\,nT}{m}$ ——— 100 nT

90°

80°

70°

60°

40°

20°

0°

S

N

sensor elevation
50 m ↕

—— 200 m ——

—— 50 m ——

—— 10 m ——

MAGNETIC FIELD
STRENGTH 50.000 nT

k = .001

k = .001

k = .005
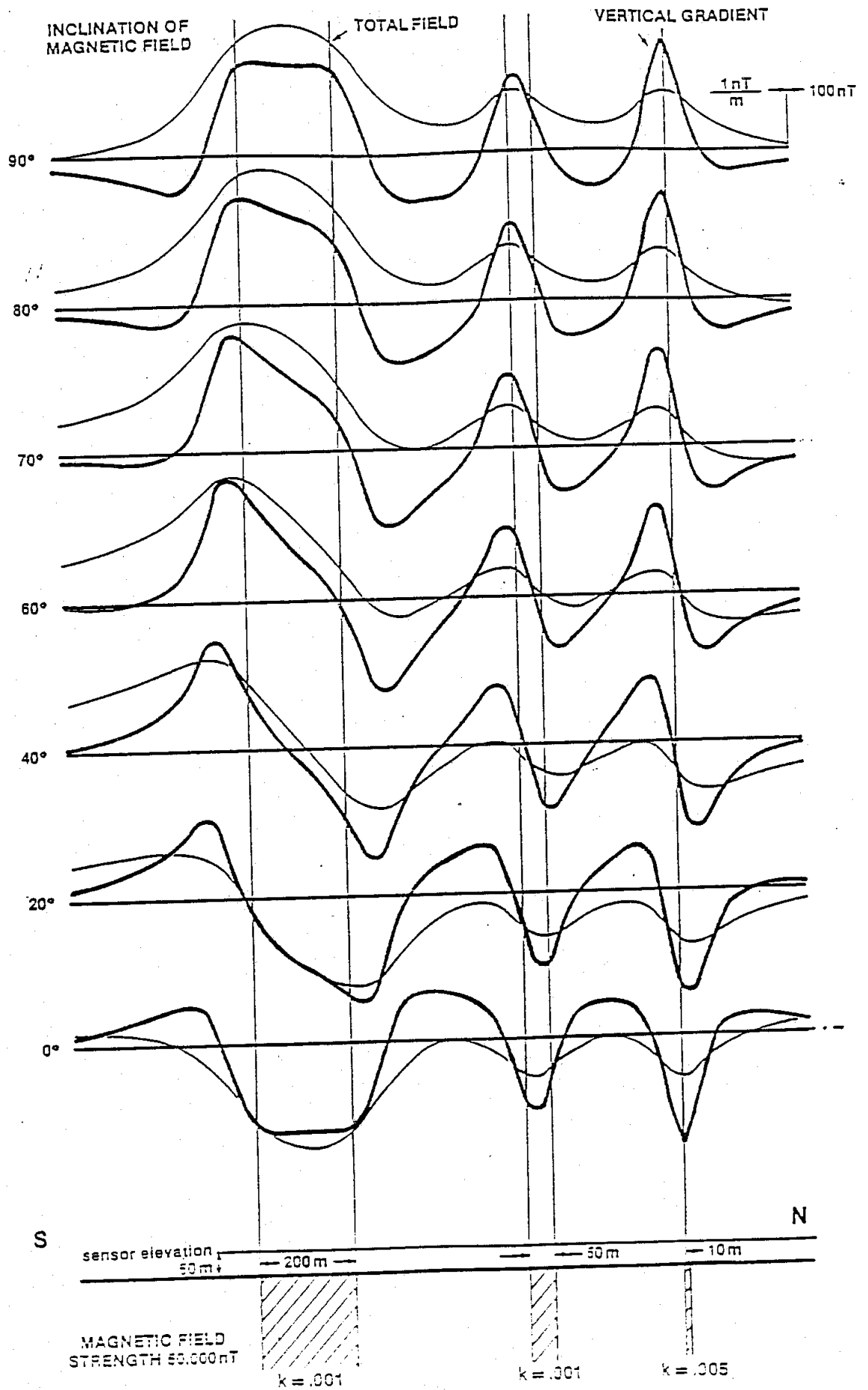
Dip

A symmetrical vertical gradient response is produced by a body dipping to magnetic north. An asymmetrical response is produced by a body which is vertical or dipping to the south. For southern dips, the southern most zero contour line may be several hundred meters south of the source.

Depth of Burial

The source-sensor separation is about equal to half of the distance between the zero contour lines for thin near-vertical sources. The estimated depth of burial for such sources is this separation minus 50 m. If a variety of VG anomaly widths are seen in an area, use the narrowest width seen to estimate local depths.

VLF Electromagnetics

The VLF-EM method employs the radiation from powerful military radio transmitters as the primary signals. The magnetic field associated with the primary field is locally horizontal and normal to a line pointing at the transmitter.

The Herz Totem uses three coils in the X, Y, Z configuration to measure the total field and vertical quadrature component from two VLF stations. These stations are designated Line and Ortho. The line station is ideally in a direction from the survey area at right angles to the flight line direction. Conductors normal to the flight line direction point at the line station and are therefore optimally coupled to VLF magnetic fields and in the best situation to gather secondary VLF currents. The ortho station is ideally 90 degrees in azimuth from the line station.

The relatively high frequency of VLF (15-25) kHz provides high response factors for bodies of low conductance. Relatively "disconnected" sulphide ores have been found to produce measurable VLF signals. For the same reason, poor conductors such as sheared contacts, breccia zones, narrow faults, alteration zones and porous flow tops normally produce VLF anomalies. The method can therefore be used effectively for geological mapping. The only relative disadvantage of the method lies in its sensitivity to conductive overburden. In conductive ground the depth of exploration is severely limited.

The effect of strike direction is important in the sense of the relation of the conductor axis relative to the energizing electromagnetic field. A conductor aligned along a radius drawn from a transmitting station will be in a maximum coupled orientation and thereby produce a stronger response than a similar conductor at a different strike angle. Theoretically, it would be possible for a conductor. oriented tangentially to the transmitter to produce no signal. The most obvious effect of the strike angle consideration is that conductors favourably oriented with respect to the transmitter location and also near perpendicular to the flight direction are most clearly rendered and usually dominate the map presentation.

The total field anomaly is an indicator of the existence and position of a conductor. The response will be a maximum over the conductor, without any special filtering, and strongly favour the upper edge of the conductor even in the case of a relatively shallow dip.

Conversely a negative total field anomaly is often seen over local resistivity highs. This is because the VLF field produces electrical currents which flow towards (or away from) the transmitter. These currents are gathered into a conductor and are taken from resistive bodies. The VLF system sees the currents gathered into the conductor as a total field high. It sees the relative absence of secondary currents in the resistor as a total field low.

As noted, VLF anomaly trends show a strong bias towards the VLF transmitter. Structure which is normal to this direction may have no associated VLF anomaly but may be seen as a break or interruption in VLF anomalies. If these structures are of particular interest, maps of the ortho station data may be worthwhile.

Conductive overburden will obscure VLF responses from bedrock sources and may produce low amplitude, broad anomalies which reflect variations in the resistivity or thickness of the overburden.

Extreme topographic relief will produce VLF anomalies which may bear no relationship to variations in electrical conductivity. Deep gullies which are too narrow to have been surveyed at a uniform sensor height often show up as VLF total field lows. Sharp ridges show up as total field highs.

The vertical quadrature component over steeply dipping sheet-like conductor will be a cross-over type response with the cross-over closely associated with the upper edge of the conductor.

The response is a cross-over type due to the fact that it is the vertical rather than total field quadrature component that is measured. The response shape is due largely to geometrical rather than conductivity considerations and the distance between the maximum and minimum on either side of the cross-over is related to target depth. For a given target geometry, the larger this distance the greater the depth.

The vertical quadrature component is rarely presented. Experience has shown the total field to be more sensitive to bedrock conductors and less affected by variations in conductive overburden.

AERODAT LIMITED
June, 1991.

APPENDIX II

ANOMALY LISTINGS

HUCKLEBERRY MTN. (AREA A)

FLIGHT	LINE	ANOMALY	CATEGORY	AMPLITUDE (PPM) INPHASE	QUAD.	CONDUCTOR MHOS	CTP DEPTH MTRS	BIRD HEIGHT MTRS		
1	10010	A	0	13.1	15.5	0.8	0	60	0.0	0.0
1	10011	A	0	-1.7	10.2	0.0	0	242	0.0	0.0
1	10020	A	0	3.6	9.1	0.1	0	224	0.0	0.0
1	10020	B	0	-254.1	17.2	0.0	0	179	0.0	0.0
1	10020	C	0	5.7	12.0	0.2	3	39	0.0	0.0
1	10020	D	0	9.8	14.3	0.5	9	34	0.0	0.0
1	10020	E	0	19.4	24.9	0.9	0	44	0.0	0.0
1	10030	A	0	-10.5	22.4	0.0	0	50	0.0	0.0
1	10030	B	0	-16.1	19.4	0.0	0	47	0.0	0.0
1	10030	C	0	-25.0	11.6	0.0	0	44	0.0	0.0
1	10030	D	0	-6.0	16.1	0.0	0	34	0.0	0.0
1	10040	A	0	-7.1	3.9	0.0	0	123	0.0	0.0
1	10040	B	0	-4.2	16.1	0.0	0	135	0.0	0.0
1	10040	C	0	4.2	10.1	0.1	0	55	0.0	0.0
1	10040	D	0	1.9	17.1	0.0	0	75	0.0	0.0
1	10050	A	1	22.7	27.6	1.0	0	117	0.0	0.0
1	10050	B	0	13.0	26.7	0.4	0	111	0.0	0.0
1	10050	C	0	8.2	15.1	0.4	0	101	0.0	0.0
1	10050	D	0	11.2	30.4	0.2	0	87	0.0	0.0
1	10050	E	0	9.1	24.3	0.2	0	78	0.0	0.0
1	10050	F	0	9.2	15.8	0.4	0	70	0.0	0.0
1	10050	G	0	11.9	21.0	0.5	0	65	0.0	0.0
1	10050	H	0	12.8	19.8	0.6	0	61	0.0	0.0
1	10050	J	0	8.5	18.1	0.3	0	54	0.0	0.0
1	10050	K	0	8.5	22.3	0.2	0	55	0.0	0.0
1	10050	M	0	-9.5	21.1	0.0	0	39	0.0	0.0
1	10060	A	0	8.9	19.6	0.3	0	87	0.0	0.0
1	10060	B	0	15.4	29.1	0.5	0	92	0.0	0.0
1	10060	C	0	17.0	25.6	0.7	0	84	0.0	0.0
2	10070	A	0	-1.4	27.1	0.0	0	62	0.0	0.0
2	10080	A	1	24.9	21.2	1.7	0	208	0.0	0.0
2	10080	B	1	29.8	30.4	1.4	0	205	0.0	0.0
2	10080	C	1	23.5	24.3	1.3	0	200	0.0	0.0
2	10080	D	1	28.6	29.4	1.4	0	188	0.0	0.0
2	10080	E	1	30.7	42.2	1.0	0	174	0.0	0.0
2	10080	F	0	-6.0	29.7	0.0	0	157	0.0	0.0

Estimated depth may be unreliable because the stronger part
of the conductor may be deeper or to one side of the flight
line, or because of a shallow dip or overburden effects.

HUCKLEBERRY MTN. (AREA A)

| FLIGHT | LINE | ANOMALY | CATEGORY | AMPLITUDE (PPM) | | CONDUCTOR | CTP DEPTH | BIRD HEIGHT |
				INPHASE	QUAD.	MHOS	MTRS	MTRS
2	10080	G	0	6.3	35.5	0.0	0	59	0.0	0.0
2	10080	H	0	8.6	16.5	0.3	0	40	0.0	0.0
2	10080	J	0	8.5	15.7	0.4	9	31	0.0	0.0
2	10080	K	0	6.7	21.1	0.1	0	47	0.0	0.0
2	10080	M	0	10.1	24.9	0.2	0	44	0.0	0.0
2	10080	N	0	14.7	29.6	0.4	0	41	0.0	0.0
2	10080	O	0	21.4	30.7	0.8	0	34	0.0	0.0
2	10090	A	0	13.7	60.1	0.1	0	106	0.0	0.0
2	10090	B	0	12.6	50.4	0.1	0	107	0.0	0.0
2	10090	C	0	11.6	45.9	0.1	0	106	0.0	0.0
2	10090	D	0	9.5	42.9	0.1	0	105	0.0	0.0
2	10090	E	0	-36.4	15.8	0.0	0	49	0.0	0.0
2	10090	F	0	-6.0	20.8	0.0	0	31	0.0	0.0
2	10090	G	0	1.9	41.2	0.0	0	29	0.0	0.0
2	10090	H	0	4.9	43.3	0.0	0	29	0.0	0.0
2	10090	J	0	-21.5	15.6	0.0	0	26	0.0	0.0
2	10090	K	0	-26.5	15.3	0.0	0	25	0.0	0.0
2	10090	M	0	-49.0	20.8	0.0	0	42	0.0	0.0
2	10090	N	0	-79.8	19.2	0.0	0	37	0.0	0.0
2	10090	O	0	24.3	44.1	0.6	0	33	0.0	0.0
2	10090	P	1	32.1	44.9	1.0	0	41	0.0	0.0
2	10090	Q	0	33.2	49.3	0.9	0	41	0.0	0.0
2	10090	R	0	18.4	42.9	0.4	0	35	0.0	0.0
2	10090	S	0	18.1	37.9	0.4	0	37	0.0	0.0
2	10090	T	0	14.9	30.4	0.4	0	39	0.0	0.0
2	10090	U	0	15.1	23.5	0.6	0	40	0.0	0.0
2	10090	V	0	11.0	15.1	0.6	0	50	0.0	0.0
2	10100	A	2	35.2	23.4	2.7	0	190	0.0	0.0
2	10100	B	1	40.6	37.1	1.9	0	191	0.0	0.0
2	10100	C	1	37.9	46.3	1.2	0	186	0.0	0.0
2	10100	D	0	14.4	69.3	0.1	0	179	0.0	0.0
2	10100	E	0	15.8	42.3	0.3	0	177	0.0	0.0
2	10100	F	0	27.5	38.3	0.9	0	166	0.0	0.0
2	10100	G	0	30.3	64.6	0.5	0	168	0.0	0.0
2	10100	H	0	-0.1	48.4	0.0	0	174	0.0	0.0
2	10100	J	0	-72.8	39.7	0.0	0	176	0.0	0.0
2	10100	K	0	-54.9	29.7	0.0	0	167	0.0	0.0
2	10101	A	0	24.9	43.2	0.6	0	75	0.0	0.0
2	10101	B	0	33.4	54.3	0.8	0	86	0.0	0.0
2	10101	C	1	34.0	39.5	1.3	0	135	0.0	0.0
2	10101	D	1	21.4	20.6	1.4	0	128	0.0	0.0
2	10101	E	0	13.7	22.0	0.6	0	121	0.0	0.0

Estimated depth may be unreliable because the stronger part
of the conductor may be deeper or to one side of the flight
line, or because of a shallow dip or overburden effects.

HUCKLEBERRY MTN. (AREA A)

FLIGHT	LINE	ANOMALY	CATEGORY	AMPLITUDE (PPM)		CONDUCTOR CTP MHOS	DEPTH MTRS	BIRD HEIGHT MTRS		
				INPHASE	QUAD.					
2	10101	F	0	11.5	22.8	0.4	1	33	0.0	0.0
2	10101	G	1	8.0	7.4	1.0	37	21	0.0	0.0
2	10101	H	0	15.9	23.0	0.7	0	42	0.0	0.0
2	10110	A	0	11.3	27.6	0.3	0	60	0.0	0.0
2	10110	B	0	3.6	25.3	0.0	0	50	0.0	0.0
2	10110	C	0	2.4	20.8	0.0	0	51	0.0	0.0
2	10110	D	0	2.1	14.3	0.0	0	52	0.0	0.0
2	10110	E	0	2.7	20.9	0.0	0	50	0.0	0.0
2	10110	F	0	4.0	28.2	0.0	0	34	0.0	0.0
2	10110	G	0	8.3	31.1	0.1	0	35	0.0	0.0
2	10110	H	0	7.2	25.9	0.1	0	31	0.0	0.0
2	10110	J	0	9.3	22.8	0.2	6	26	0.0	0.0
2	10110	K	0	7.8	20.1	0.2	9	24	0.0	0.0
2	10110	M	0	13.7	22.2	0.5	12	24	0.0	0.0
2	10110	N	0	8.9	22.5	0.2	6	26	0.0	0.0
2	10110	O	0	8.3	23.5	0.2	3	27	0.0	0.0
2	10110	P	0	16.4	47.3	0.2	0	28	0.0	0.0
2	10110	Q	0	10.0	36.8	0.1	0	26	0.0	0.0
2	10110	R	0	4.6	24.9	0.0	0	25	0.0	0.0
2	10110	S	0	6.7	36.5	0.0	0	33	0.0	0.0
2	10110	T	0	21.9	47.0	0.4	0	31	0.0	0.0
2	10110	U	1	48.9	47.9	1.8	1	29	0.0	0.0
2	10110	V	1	54.1	63.8	1.5	0	26	0.0	0.0
2	10110	W	1	58.1	66.2	1.6	0	26	0.0	0.0
2	10110	X	0	46.0	85.9	0.7	0	31	0.0	0.0
2	10110	Y	0	33.1	69.5	0.6	0	32	0.0	0.0
2	10110	Z	0	18.1	55.5	0.2	0	35	0.0	0.0
2	10110	AA	0	19.6	61.2	0.2	0	37	0.0	0.0
2	10110	AB	0	22.8	43.8	0.5	0	29	0.0	0.0
2	10110	AC	0	17.3	33.7	0.5	5	25	0.0	0.0
2	10110	AD	0	17.4	36.8	0.4	1	27	0.0	0.0
2	10110	AE	0	8.4	36.5	0.1	0	30	0.0	0.0
2	10110	AF	0	-8.4	28.7	0.0	0	36	0.0	0.0
2	10110	AG	0	-135.5	34.6	0.0	0	32	0.0	0.0
2	10110	AH	0	-203.6	39.6	0.0	0	36	0.0	0.0
2	10110	AJ	0	-308.4	59.9	0.0	0	43	0.0	0.0
2	10120	A	0	17.1	21.2	0.9	0	332	0.0	0.0
2	10120	B	0	18.3	36.1	0.5	0	321	0.0	0.0
2	10120	C	0	18.3	25.1	0.8	0	315	0.0	0.0
2	10120	D	1	18.9	15.9	1.6	0	300	0.0	0.0
2	10120	E	1	28.1	23.5	1.8	0	294	0.0	0.0
2	10120	F	1	30.5	39.9	1.0	0	283	0.0	0.0
2	10120	G	0	64.7	132.9	0.8	0	289	0.0	0.0

Estimated depth may be unreliable because the stronger part
of the conductor may be deeper or to one side of the flight
line, or because of a shallow dip or overburden effects.

HUCKLEBERRY MTN. (AREA A)

FLIGHT	LINE	ANOMALY	CATEGORY	AMPLITUDE (PPM) INPHASE	QUAD.	CONDUCTOR CTP MHOS	DEPTH MTRS	BIRD HEIGHT MTRS		
2	10120	H	0	35.2	63.5	0.7	0	277	0.0	0.0
2	10120	J	0	14.2	34.0	0.3	0	239	0.0	0.0
2	10120	K	0	17.2	41.2	0.3	0	202	0.0	0.0
2	10120	M	0	9.0	56.6	0.0	0	189	0.0	0.0
2	10120	N	0	4.3	29.0	0.0	0	163	0.0	0.0
2	10120	O	0	-2.6	32.3	0.0	0	154	0.0	0.0
2	10120	P	0	9.4	19.0	0.3	0	150	0.0	0.0
2	10120	Q	0	14.5	23.7	0.6	0	143	0.0	0.0
2	10120	R	0	18.2	26.7	0.7	0	101	0.0	0.0
2	10120	S	0	10.6	20.0	0.4	0	90	0.0	0.0
2	10120	T	0	13.8	22.9	0.5	0	37	0.0	0.0
2	10120	U	0	11.1	21.5	0.4	2	33	0.0	0.0
2	10120	V	0	7.9	20.0	0.2	1	32	0.0	0.0
2	10120	W	0	12.7	24.2	0.4	0	36	0.0	0.0
2	10120	X	0	8.8	15.4	0.4	7	33	0.0	0.0
2	10120	Y	0	5.4	11.8	0.2	0	64	0.0	0.0
2	10120	Z	0	4.4	15.2	0.1	0	51	0.0	0.0
2	10130	A	0	2.9	15.1	0.0	0	85	0.0	0.0
2	10130	B	0	10.2	25.9	0.2	0	71	0.0	0.0
2	10130	C	0	1.9	21.0	0.0	0	41	0.0	0.0
2	10130	D	0	4.9	27.2	0.0	0	41	0.0	0.0
2	10130	E	0	3.1	26.8	0.0	0	41	0.0	0.0
2	10130	F	0	-1.1	22.4	0.0	0	42	0.0	0.0
2	10130	G	0	9.4	32.3	0.1	0	47	0.0	0.0
2	10130	H	0	15.8	25.3	0.6	0	49	0.0	0.0
2	10130	J	0	12.7	30.4	0.3	0	34	0.0	0.0
2	10130	K	0	12.1	21.4	0.5	0	36	0.0	0.0
2	10130	M	0	10.0	26.2	0.2	0	39	0.0	0.0
2	10130	N	0	14.5	24.0	0.5	0	49	0.0	0.0
2	10130	O	1	32.4	35.0	1.4	0	47	0.0	0.0
2	10130	P	1	22.8	22.3	1.4	1	38	0.0	0.0
2	10130	Q	1	23.7	24.1	1.3	5	33	0.0	0.0
2	10130	R	0	27.5	49.8	0.6	0	37	0.0	0.0
2	10130	S	0	36.6	68.8	0.7	0	34	0.0	0.0
2	10130	T	0	-3.5	37.9	0.0	0	32	0.0	0.0
2	10130	U	0	7.0	29.6	0.1	0	34	0.0	0.0
2	10130	V	0	7.0	30.2	0.1	0	30	0.0	0.0
2	10130	W	0	7.1	27.3	0.1	0	32	0.0	0.0
2	10130	X	0	15.6	48.3	0.2	0	29	0.0	0.0
2	10130	Y	0	-10.2	27.9	0.0	0	34	0.0	0.0
2	10140	A	0	8.3	40.8	0.1	0	282	0.0	0.0
2	10140	B	1	73.7	109.4	1.2	0	288	0.0	0.0
2	10140	C	1	77.0	92.2	1.6	0	284	0.0	0.0

Estimated depth may be unreliable because the stronger part
of the conductor may be deeper or to one side of the flight
line, or because of a shallow dip or overburden effects.

HUCKLEBERRY MTN. (AREA A)

FLIGHT	LINE	ANOMALY	CATEGORY	AMPLITUDE (PPM)		CONDUCTOR MHOS	CTP DEPTH MTRS	BIRD HEIGHT MTRS		
				INPHASE	QUAD.					
2	10140	D	0	41.2	68.2	0.8	0	202	0.0	0.0
2	10140	E	0	31.8	83.8	0.4	0	193	0.0	0.0
2	10140	F	1	45.8	54.7	1.4	0	183	0.0	0.0
2	10140	G	1	45.9	54.8	1.4	0	174	0.0	0.0
2	10140	H	0	-9.1	111.2	0.0	0	156	0.0	0.0
2	10140	J	1	26.0	34.3	1.0	0	132	0.0	0.0
2	10140	K	0	23.4	50.8	0.5	0	92	0.0	0.0
2	10140	M	0	15.1	18.5	0.9	0	72	0.0	0.0
2	10140	N	1	17.1	19.4	1.0	0	42	0.0	0.0
2	10140	O	0	11.3	15.3	0.7	8	35	0.0	0.0
2	10140	P	0	9.1	13.3	0.5	8	36	0.0	0.0
2	10140	Q	0	6.1	23.2	0.1	0	57	0.0	0.0
2	10140	R	0	4.7	25.0	0.0	0	56	0.0	0.0
2	10140	S	0	5.3	19.1	0.1	0	55	0.0	0.0
2	10140	T	0	2.9	14.4	0.0	0	49	0.0	0.0
2	10150	A	0	12.4	25.5	0.4	1	31	0.0	0.0
2	10150	B	0	16.0	21.7	0.8	1	37	0.0	0.0
2	10150	C	0	9.2	16.1	0.4	6	34	0.0	0.0
2	10150	D	0	7.9	19.7	0.2	0	36	0.0	0.0
2	10150	E	0	9.7	16.1	0.4	1	39	0.0	0.0
2	10150	F	0	9.1	18.1	0.3	0	39	0.0	0.0
2	10150	G	0	9.2	16.8	0.4	1	38	0.0	0.0
2	10150	H	0	8.0	24.7	0.1	0	39	0.0	0.0
2	10150	J	0	6.6	42.3	0.0	0	38	0.0	0.0
2	10150	K	0	-5.3	23.2	0.0	0	37	0.0	0.0
2	10150	M	0	5.5	44.8	0.0	0	45	0.0	0.0
2	10150	N	0	2.1	49.3	0.0	0	44	0.0	0.0
2	10150	O	0	12.9	41.7	0.2	0	41	0.0	0.0
2	10150	P	0	-0.1	58.0	0.0	0	38	0.0	0.0
2	10150	Q	0	-15.5	60.8	0.0	0	39	0.0	0.0
2	10150	R	0	-15.7	36.4	0.0	0	33	0.0	0.0
2	10150	S	0	23.5	70.2	0.3	0	37	0.0	0.0
2	10150	T	0	27.6	61.5	0.5	0	38	0.0	0.0
2	10150	U	0	32.0	50.5	0.8	0	34	0.0	0.0
2	10150	V	1	53.5	85.7	1.0	0	39	0.0	0.0
2	10150	W	0	34.9	60.8	0.7	0	34	0.0	0.0
2	10150	X	0	30.6	138.0	0.2	0	33	0.0	0.0
2	10150	Y	0	56.1	235.4	0.3	0	30	0.0	0.0
2	10150	Z	0	-85.1	531.7	0.0	0	27	0.0	0.0
2	10150	AA	0	13.0	38.2	0.2	0	39	0.0	0.0
2	10150	AB	0	11.3	31.7	0.2	0	36	0.0	0.0
2	10150	AC	0	13.9	44.8	0.2	0	35	0.0	0.0
2	10160	A	0	26.1	62.5	0.4	0	280	0.0	0.0

Estimated depth may be unreliable because the stronger part
of the conductor may be deeper or to one side of the flight
line, or because of a shallow dip or overburden effects.

HUCKLEBERRY MTN. (AREA A)

FLIGHT	LINE	ANOMALY	CATEGORY	AMPLITUDE (PPM)		CONDUCTOR MHOS	CTP DEPTH MTRS	BIRD HEIGHT MTRS		
				INPHASE	QUAD.					
2	10160	B	0	39.4	105.2	0.4	0	269	0.0	0.0
2	10160	C	0	36.0	86.2	0.5	0	266	0.0	0.0
2	10160	D	0	15.8	54.5	0.2	0	261	0.0	0.0
2	10160	E	0	13.9	26.3	0.4	0	245	0.0	0.0
2	10160	F	0	23.7	34.7	0.8	0	239	0.0	0.0
2	10160	G	0	24.6	41.9	0.7	0	234	0.0	0.0
2	10160	H	0	28.5	60.7	0.5	0	227	0.0	0.0
2	10160	J	0	13.3	43.5	0.2	0	221	0.0	0.0
2	10160	K	0	10.3	30.5	0.2	0	216	0.0	0.0
2	10160	M	0	5.7	14.2	0.2	0	203	0.0	0.0
2	10160	N	0	9.0	14.0	0.5	0	186	0.0	0.0
2	10160	O	0	9.1	13.7	0.5	0	178	0.0	0.0
2	10160	P	0	9.6	18.8	0.3	0	157	0.0	0.0
2	10160	Q	0	11.6	34.9	0.2	0	150	0.0	0.0
2	10160	R	0	15.2	45.2	0.2	0	144	0.0	0.0
2	10160	S	0	12.8	41.4	0.2	0	138	0.0	0.0
2	10160	T	0	6.8	12.4	0.3	0	126	0.0	0.0
2	10160	U	0	0.4	14.7	0.0	0	121	0.0	0.0
2	10160	V	0	12.0	14.1	0.8	0	86	0.0	0.0
2	10160	W	1	19.5	18.5	1.3	0	78	0.0	0.0
2	10160	X	1	27.8	31.0	1.2	0	59	0.0	0.0
2	10160	Y	0	23.2	32.5	0.8	0	54	0.0	0.0
2	10160	Z	0	12.2	20.5	0.5	0	47	0.0	0.0
2	10160	AA	0	3.6	18.9	0.0	0	37	0.0	0.0
2	10160	AB	1	33.6	44.4	1.1	0	32	0.0	0.0
3	10170	A	0	21.0	33.5	0.7	0	97	0.0	0.0
3	10170	B	1	26.4	30.7	1.1	0	95	0.0	0.0
3	10170	C	1	19.5	21.0	1.1	0	99	0.0	0.0
3	10170	D	1	27.9	28.4	1.4	0	45	0.0	0.0
3	10170	E	2	31.2	25.2	2.0	0	46	0.0	0.0
3	10170	F	0	8.4	24.6	0.2	0	46	0.0	0.0
3	10170	G	0	9.5	21.1	0.3	0	43	0.0	0.0
3	10170	H	0	9.4	17.8	0.4	0	46	0.0	0.0
3	10170	J	0	8.8	18.9	0.3	0	45	0.0	0.0
3	10170	K	0	-0.7	35.8	0.0	0	34	0.0	0.0
3	10170	M	0	6.2	39.9	0.0	0	33	0.0	0.0
3	10170	N	0	7.6	27.0	0.1	0	33	0.0	0.0
3	10170	O	0	0.9	22.9	0.0	0	36	0.0	0.0
3	10170	P	0	0.2	36.8	0.0	0	36	0.0	0.0
3	10170	Q	0	7.0	33.5	0.0	0	37	0.0	0.0
3	10171	A	0	-8.1	18.9	0.0	0	70	0.0	0.0
3	10180	A	0	20.4	33.1	0.7	0	177	0.0	0.0

Estimated depth may be unreliable because the stronger part
of the conductor may be deeper or to one side of the flight
line, or because of a shallow dip or overburden effects.

HUCKLEBERRY MTN. (AREA A)

FLIGHT	LINE	ANOMALY	CATEGORY	AMPLITUDE (PPM) INPHASE	QUAD.	CONDUCTOR MHOS	CTP MTRS	DEPTH MTRS	BIRD HEIGHT MTRS	
3	10180	B	0	20.1	25.8	0.9	0	173	0.0	0.0
3	10180	C	0	17.0	25.3	0.7	0	171	0.0	0.0
3	10180	D	0	-0.8	36.7	0.0	0	170	0.0	0.0
3	10180	E	0	-7.3	33.2	0.0	0	169	0.0	0.0
3	10180	F	0	-10.0	34.0	0.0	0	164	0.0	0.0
3	10180	G	0	-1.8	41.1	0.0	0	160	0.0	0.0
3	10180	H	0	-3.0	44.2	0.0	0	157	0.0	0.0
3	10180	J	0	-7.5	60.5	0.0	0	155	0.0	0.0
3	10180	K	0	1.8	65.5	0.0	0	153	0.0	0.0
3	10180	M	0	-3.1	58.3	0.0	0	151	0.0	0.0
3	10180	N	1	11.9	11.5	1.1	0	82	0.0	0.0
3	10180	O	1	17.5	20.5	1.0	0	59	0.0	0.0
3	10180	P	1	18.4	21.1	1.0	0	57	0.0	0.0
3	10180	Q	0	19.3	30.6	0.7	0	50	0.0	0.0
3	10180	R	0	15.8	24.8	0.6	0	44	0.0	0.0
3	10180	S	0	-0.8	4.6	0.0	0	23	0.0	0.0
3	10180	T	1	38.0	38.0	1.6	0	37	0.0	0.0
3	10180	U	1	41.2	39.9	1.7	0	35	0.0	0.0
3	10180	V	1	26.4	30.2	1.2	1	34	0.0	0.0
3	10180	W	1	31.8	43.7	1.0	0	33	0.0	0.0
3	10180	X	1	33.6	44.4	1.1	0	33	0.0	0.0
3	10180	Y	0	19.1	25.7	0.8	4	32	0.0	0.0
3	10190	A	0	23.8	53.4	0.4	0	31	0.0	0.0
3	10190	B	0	29.4	58.6	0.6	0	31	0.0	0.0
3	10190	C	0	30.6	56.9	0.6	0	31	0.0	0.0
3	10190	D	0	29.7	66.2	0.5	0	32	0.0	0.0
3	10190	E	0	28.7	63.5	0.5	0	32	0.0	0.0
3	10190	F	0	10.4	21.4	0.3	3	31	0.0	0.0
3	10190	G	0	19.0	35.9	0.5	0	39	0.0	0.0
3	10190	H	0	-42.9	4.8	0.0	0	33	0.0	0.0
3	10190	J	0	8.2	19.7	0.2	3	31	0.0	0.0
3	10190	K	0	-51.4	15.4	0.0	0	27	0.0	0.0
3	10190	M	0	-8.2	14.3	0.0	0	25	0.0	0.0
3	10190	N	0	3.5	29.5	0.0	0	24	0.0	0.0
3	10190	O	0	5.5	25.0	0.0	0	28	0.0	0.0
3	10190	P	0	3.5	25.5	0.0	0	31	0.0	0.0
3	10190	Q	0	3.1	31.7	0.0	0	36	0.0	0.0
3	10190	R	0	7.8	31.9	0.1	0	37	0.0	0.0
3	10190	S	0	6.3	21.3	0.1	0	38	0.0	0.0
3	10190	T	0	4.4	18.3	0.0	0	38	0.0	0.0
3	10190	U	0	-7.7	26.3	0.0	0	33	0.0	0.0
3	10190	V	0	-18.6	13.4	0.0	0	25	0.0	0.0
3	10200	A	0	15.2	49.6	0.2	0	165	0.0	0.0

Estimated depth may be unreliable because the stronger part
of the conductor may be deeper or to one side of the flight
line, or because of a shallow dip or overburden effects.

HUCKLEBERRY MTN. (AREA A)

FLIGHT	LINE	ANOMALY	CATEGORY	AMPLITUDE (PPM)		CONDUCTOR	CTP DEPTH	BIRD HEIGHT		
				INPHASE	QUAD.	MHOS	MTRS	MTRS		
3	10200	B	0	7.2	22.7	0.1	0	156	0.0	0.0
3	10200	C	0	17.3	28.5	0.6	0	120	0.0	0.0
3	10200	D	1	25.2	31.2	1.0	0	113	0.0	0.0
3	10200	E	0	25.6	39.2	0.8	0	106	0.0	0.0
3	10200	F	1	25.8	29.8	1.1	0	97	0.0	0.0
3	10200	G	1	23.3	24.8	1.2	0	84	0.0	0.0
3	10200	H	0	8.8	20.3	0.3	0	52	0.0	0.0
3	10200	J	0	12.1	15.3	0.7	0	44	0.0	0.0
3	10200	K	0	9.3	18.7	0.3	0	47	0.0	0.0
3	10200	M	0	-5.5	15.2	0.0	0	52	0.0	0.0
3	10200	N	0	-3.7	20.3	0.0	0	61	0.0	0.0
3	10200	O	0	-3.2	12.2	0.0	0	69	0.0	0.0
3	10200	P	0	9.2	11.6	0.7	0	51	0.0	0.0
3	10200	Q	0	10.0	19.8	0.3	0	47	0.0	0.0
3	10200	R	0	10.4	19.9	0.4	0	44	0.0	0.0
3	10200	S	0	15.0	19.6	0.8	4	35	0.0	0.0
3	10200	T	1	22.1	27.3	1.0	9	26	0.0	0.0
3	10200	U	0	23.0	33.0	0.8	10	22	0.0	0.0
3	10200	V	0	21.3	39.8	0.5	8	20	0.0	0.0
3	10200	W	0	-14.5	10.9	0.0	0	20	0.0	0.0
3	10200	X	0	8.5	16.2	0.3	5	34	0.0	0.0
3	10200	Y	0	8.0	11.4	0.5	2	45	0.0	0.0
3	10200	Z	0	10.8	18.9	0.4	0	45	0.0	0.0
3	10200	AA	0	17.2	28.0	0.6	0	52	0.0	0.0
3	10200	AB	0	17.7	29.7	0.6	0	52	0.0	0.0
3	10210	A	0	0.4	15.0	0.0	0	41	0.0	0.0
3	10210	B	0	0.2	16.4	0.0	0	40	0.0	0.0
3	10210	C	0	5.2	14.6	0.1	5	31	0.0	0.0
3	10210	D	0	5.7	16.0	0.1	11	24	0.0	0.0
3	10210	E	0	5.3	13.5	0.2	10	28	0.0	0.0
3	10210	F	0	3.2	16.0	0.0	2	27	0.0	0.0
3	10210	G	0	-11.8	11.1	0.0	0	33	0.0	0.0
3	10210	H	0	14.4	22.3	0.6	15	21	0.0	0.0
3	10210	J	0	16.8	22.8	0.8	16	21	0.0	0.0
3	10220	A	0	-8.8	9.7	0.0	0	212	0.0	0.0
3	10220	B	0	-0.6	17.9	0.0	0	172	0.0	0.0
3	10220	C	0	1.2	20.9	0.0	0	140	0.0	0.0
3	10220	D	0	1.5	28.8	0.0	0	135	0.0	0.0
3	10220	E	0	8.9	19.8	0.3	0	119	0.0	0.0
3	10220	F	0	-7.6	13.7	0.0	0	121	0.0	0.0
3	10220	G	0	-1.3	12.1	0.0	0	44	0.0	0.0
3	10220	H	0	2.5	13.9	0.0	15	15	0.0	0.0
3	10230	A	0	-3.0	19.5	0.0	0	36	0.0	0.0

Estimated depth may be unreliable because the stronger part
of the conductor may be deeper or to one side of the flight
line, or because of a shallow dip or overburden effects.

HUCKLEBERRY MTN. (AREA A)

FLIGHT	LINE	ANOMALY	CATEGORY	AMPLITUDE (PPM)		CONDUCTOR MHOS	CTP DEPTH MTRS	BIRD HEIGHT MTRS		
				INPHASE	QUAD.					
3	10230	B	0	4.2	32.0	0.0	0	35	0.0	0.0
3	10230	C	0	6.5	33.4	0.0	0	35	0.0	0.0
3	10230	D	0	4.8	28.0	0.0	0	35	0.0	0.0
3	10230	E	0	-0.3	37.8	0.0	0	35	0.0	0.0
3	10230	F	0	6.6	24.9	0.1	0	28	0.0	0.0
3	10230	G	0	2.5	12.9	0.0	1	30	0.0	0.0
3	10230	H	0	2.2	10.6	0.0	0	42	0.0	0.0
3	10230	J	0	-1.8	12.9	0.0	0	41	0.0	0.0
3	10240	A	0	-2.8	10.5	0.0	0	143	0.0	0.0
3	10240	B	0	-6.8	16.5	0.0	0	139	0.0	0.0
3	10240	C	0	7.2	25.0	0.1	0	90	0.0	0.0
3	10240	D	0	-9.8	17.7	0.0	0	117	0.0	0.0
3	10240	E	0	-0.6	12.9	0.0	0	70	0.0	0.0
3	10240	F	0	0.7	9.0	0.0	0	29	0.0	0.0
3	10240	G	0	7.1	25.5	0.1	7	20	0.0	0.0
3	10240	H	0	4.3	14.9	0.1	15	19	0.0	0.0
3	10240	J	0	-12.4	24.3	0.0	0	36	0.0	0.0
3	10240	K	0	5.8	24.1	0.1	0	27	0.0	0.0
3	10240	M	0	14.6	35.8	0.3	0	28	0.0	0.0
3	10240	N	0	19.6	42.3	0.4	1	26	0.0	0.0
3	10240	O	0	11.5	19.5	0.5	14	23	0.0	0.0
3	10250	A	0	23.1	40.2	0.6	0	85	0.0	0.0
3	10250	B	0	29.4	52.6	0.7	0	86	0.0	0.0
3	10260	A	0	-31.2	16.3	0.0	0	61	0.0	0.0
3	10260	B	0	15.0	23.0	0.6	0	36	0.0	0.0
3	10260	C	0	-0.1	25.8	0.0	0	31	0.0	0.0
3	10260	D	0	-13.2	13.3	0.0	0	43	0.0	0.0
3	10260	E	0	-1.2	13.6	0.0	0	45	0.0	0.0
4	10270	A	0	10.8	22.2	0.3	0	164	0.0	0.0
4	10270	B	0	10.7	17.6	0.5	0	161	0.0	0.0
4	10280	A	0	4.1	20.6	0.0	0	72	0.0	0.0
4	10280	B	0	2.2	21.3	0.0	0	68	0.0	0.0
4	10280	C	0	10.4	23.2	0.3	0	114	0.0	0.0
4	10280	D	0	14.5	30.1	0.4	0	112	0.0	0.0
4	10280	E	0	12.0	19.3	0.5	0	109	0.0	0.0
4	10280	F	0	3.6	15.5	0.0	0	61	0.0	0.0
4	10280	G	0	-7.5	17.7	0.0	0	53	0.0	0.0
4	10280	H	0	-15.3	19.1	0.0	0	48	0.0	0.0
4	10280	J	0	-9.8	22.3	0.0	0	42	0.0	0.0
4	10280	K	0	-9.7	24.2	0.0	0	44	0.0	0.0

Estimated depth may be unreliable because the stronger part
of the conductor may be deeper or to one side of the flight
line, or because of a shallow dip or overburden effects.

HUCKLEBERRY MTN. (AREA A)

FLIGHT	LINE	ANOMALY	CATEGORY	AMPLITUDE (PPM) INPHASE	QUAD.	CONDUCTOR MHOS	CTP DEPTH MTRS	BIRD HEIGHT MTRS		
4	10280	M	0	17.2	23.0	0.8	3	34	0.0	0.0
4	10280	N	0	19.4	32.6	0.6	0	34	0.0	0.0
4	10280	O	0	28.0	54.8	0.6	0	33	0.0	0.0
4	10280	P	0	30.3	48.9	0.8	0	32	0.0	0.0
4	10280	Q	0	8.5	43.2	0.0	0	31	0.0	0.0
4	10290	A	0	5.1	22.2	0.0	0	44	0.0	0.0
4	10290	B	1	22.3	26.7	1.0	0	42	0.0	0.0
4	10290	C	0	18.2	26.5	0.7	0	43	0.0	0.0
4	10290	D	0	19.0	28.0	0.7	0	47	0.0	0.0
4	10290	E	0	18.0	30.1	0.6	0	47	0.0	0.0
4	10300	A	0	8.9	17.5	0.3	0	57	0.0	0.0
4	10300	B	0	7.8	28.3	0.1	0	49	0.0	0.0
4	10300	C	0	12.1	16.6	0.7	2	39	0.0	0.0
4	10300	D	0	10.7	17.2	0.5	0	48	0.0	0.0
4	10300	E	0	11.2	19.0	0.5	0	47	0.0	0.0
4	10300	F	0	8.9	16.5	0.4	0	49	0.0	0.0
4	10300	G	0	-31.5	11.2	0.0	0	44	0.0	0.0
4	10300	H	0	-17.4	27.3	0.0	0	42	0.0	0.0
4	10300	J	0	12.5	22.2	0.5	0	37	0.0	0.0
4	10300	K	0	20.3	32.2	0.7	0	40	0.0	0.0
4	10300	M	1	21.4	23.3	1.2	0	46	0.0	0.0
5	10310	A	0	14.9	19.2	0.8	0	67	0.0	0.0
5	10310	B	0	13.0	14.8	0.9	0	62	0.0	0.0
5	10310	C	0	11.6	21.8	0.4	0	45	0.0	0.0
5	10310	D	0	13.3	32.1	0.3	0	49	0.0	0.0
5	10310	E	0	9.1	29.5	0.1	0	51	0.0	0.0
5	10310	F	0	4.2	27.3	0.0	0	60	0.0	0.0
5	10320	A	0	5.9	15.6	0.2	0	40	0.0	0.0
5	10320	B	0	14.9	20.5	0.7	0	40	0.0	0.0
5	10320	C	0	15.4	26.7	0.5	0	54	0.0	0.0
5	10320	D	0	13.7	26.3	0.4	0	54	0.0	0.0
5	10320	E	0	12.6	16.4	0.7	0	46	0.0	0.0
5	10320	F	0	16.0	34.6	0.4	0	48	0.0	0.0
5	10320	G	0	31.9	124.1	0.2	0	50	0.0	0.0
5	10320	H	0	32.0	166.8	0.1	0	49	0.0	0.0
5	10320	J	0	37.0	102.4	0.4	0	50	0.0	0.0
5	10320	K	0	8.8	30.5	0.1	0	46	0.0	0.0
5	10320	M	0	1.7	22.9	0.0	0	57	0.0	0.0
5	10320	N	0	-7.6	15.4	0.0	0	34	0.0	0.0
5	10330	A	0	11.4	21.0	0.4	0	60	0.0	0.0

Estimated depth may be unreliable because the stronger part
of the conductor may be deeper or to one side of the flight
line, or because of a shallow dip or overburden effects.

HUCKLEBERRY MTN. (AREA A)

FLIGHT	LINE	ANOMALY	CATEGORY	AMPLITUDE (PPM) INPHASE	QUAD.	CONDUCTOR CTP MHOS	DEPTH MTRS	BIRD HEIGHT MTRS		
5	10330	B	0	3.9	29.7	0.0	0	60	0.0	0.0
5	10330	C	0	9.2	42.9	0.1	0	54	0.0	0.0
5	10330	D	0	9.6	29.4	0.2	0	49	0.0	0.0
5	10330	E	0	7.6	12.5	0.4	5	39	0.0	0.0
5	10330	F	0	5.0	37.6	0.0	0	61	0.0	0.0
5	10330	G	0	12.9	44.1	0.2	0	62	0.0	0.0
5	10340	A	0	7.0	37.3	0.0	0	47	0.0	0.0
5	10340	B	0	5.4	18.7	0.1	0	54	0.0	0.0
5	10340	C	1	13.7	14.1	1.0	0	48	0.0	0.0
5	10340	D	0	2.3	28.9	0.0	0	96	0.0	0.0
5	10340	E	0	11.3	60.3	0.1	0	92	0.0	0.0
5	10340	F	0	2.8	37.5	0.0	0	67	0.0	0.0
5	10340	G	0	-9.8	42.5	0.0	0	59	0.0	0.0
5	10350	A	0	31.9	47.5	0.9	0	81	0.0	0.0
5	10350	B	0	23.5	34.1	0.8	0	80	0.0	0.0
5	10350	C	0	16.9	26.0	0.6	0	75	0.0	0.0
5	10350	D	0	8.8	12.9	0.5	0	45	0.0	0.0
5	10350	E	0	14.5	21.4	0.6	0	44	0.0	0.0
5	10350	F	0	4.6	25.6	0.0	0	44	0.0	0.0
5	10350	G	0	9.2	39.7	0.1	0	41	0.0	0.0
5	10350	H	0	6.7	19.7	0.1	0	43	0.0	0.0
5	10360	A	0	3.9	20.7	0.0	0	71	0.0	0.0
5	10360	B	0	9.7	54.1	0.0	0	69	0.0	0.0
5	10360	C	0	12.7	49.7	0.1	0	68	0.0	0.0
5	10360	D	0	8.1	38.0	0.1	0	67	0.0	0.0
5	10360	E	0	1.6	13.3	0.0	0	41	0.0	0.0
5	10360	F	0	-2.0	17.4	0.0	0	49	0.0	0.0
5	10360	G	0	12.2	16.0	0.7	0	49	0.0	0.0
5	10370	A	0	24.2	36.0	0.8	0	50	0.0	0.0
5	10370	B	0	14.0	20.4	0.6	0	58	0.0	0.0
5	10370	C	0	2.8	13.8	0.0	0	39	0.0	0.0
5	10370	D	0	4.8	15.0	0.1	0	39	0.0	0.0
5	10370	E	0	5.1	23.6	0.0	0	40	0.0	0.0
5	10370	F	0	5.0	25.2	0.0	0	41	0.0	0.0
5	10380	A	0	1.1	10.4	0.0	0	59	0.0	0.0
5	10380	B	0	9.8	22.3	0.3	0	42	0.0	0.0
5	10380	C	0	15.2	22.8	0.6	0	40	0.0	0.0
5	10400	A	0	7.0	25.1	0.1	0	43	0.0	0.0
5	10400	B	0	18.5	36.5	0.5	0	46	0.0	0.0

Estimated depth may be unreliable because the stronger part
of the conductor may be deeper or to one side of the flight
line, or because of a shallow dip or overburden effects.

HUCKLEBERRY MTN. (AREA A)

FLIGHT	LINE	ANOMALY	CATEGORY	AMPLITUDE (PPM) INPHASE	QUAD.	CONDUCTOR CTP MHOS	DEPTH MTRS	BIRD HEIGHT MTRS		
5	10400	C	0	5.1	26.1	0.0	0	36	0.0	0.0
5	10400	D	0	0.9	16.3	0.0	0	41	0.0	0.0
6	10430	A	0	8.2	19.0	0.2	0	41	0.0	0.0
6	10430	B	0	-1.1	16.8	0.0	0	40	0.0	0.0
6	10430	C	0	-2.0	17.3	0.0	0	40	0.0	0.0
6	10440	A	0	6.5	18.0	0.2	0	57	0.0	0.0
6	10440	B	0	12.4	25.2	0.4	0	48	0.0	0.0
6	10440	C	0	13.4	26.3	0.4	0	47	0.0	0.0
6	10440	D	3	14.5	5.3	4.5	15	44	0.0	0.0
6	10440	E	1	21.9	23.5	1.2	0	38	0.0	0.0
6	10450	A	1	18.5	15.7	1.5	0	101	0.0	0.0
6	10450	B	2	16.2	10.2	2.2	0	88	0.0	0.0
6	10450	C	0	5.9	13.8	0.2	0	63	0.0	0.0
6	10450	D	0	7.0	17.8	0.2	0	60	0.0	0.0
6	10460	A	0	7.6	22.7	0.1	0	35	0.0	0.0
6	10460	B	0	5.1	16.3	0.1	0	38	0.0	0.0
6	10460	C	0	8.8	12.9	0.5	2	43	0.0	0.0
6	10460	D	2	18.7	10.7	2.7	17	33	0.0	0.0
6	10460	E	2	17.9	8.6	3.3	20	33	0.0	0.0
6	10460	F	0	11.1	15.0	0.6	3	40	0.0	0.0

HUCKLEBERRY MTN. (AREA B)

FLIGHT	LINE	ANOMALY	CATEGORY	AMPLITUDE (PPM)		CONDUCTOR CTP MHOS	DEPTH MTRS	BIRD HEIGHT MTRS		
				INPHASE	QUAD.					
7	20010	A	0	4.4	7.6	0.3	11	41	0.0	0.0
7	20010	B	0	6.4	9.5	0.4	10	40	0.0	0.0
7	20010	C	0	6.9	10.3	0.4	7	41	0.0	0.0
7	20010	D	0	5.6	8.8	0.4	10	41	0.0	0.0
7	20010	E	0	4.4	10.8	0.1	1	41	0.0	0.0
7	20010	F	0	2.5	5.6	0.1	13	41	0.0	0.0
7	20010	G	0	16.0	36.9	0.3	0	46	0.0	0.0
7	20010	H	0	11.7	40.9	0.1	0	42	0.0	0.0
7	20010	J	0	11.1	33.4	0.2	0	41	0.0	0.0
7	20010	K	0	6.5	14.0	0.2	0	40	0.0	0.0
7	20010	M	0	6.8	29.3	0.1	0	38	0.0	0.0
7	20020	A	0	3.7	8.4	0.2	0	76	0.0	0.0
7	20020	B	0	6.7	6.6	0.8	0	60	0.0	0.0
7	20020	C	0	10.9	15.4	0.6	0	58	0.0	0.0
7	20020	D	0	14.1	19.5	0.7	0	55	0.0	0.0
7	20020	E	0	4.9	5.2	0.6	12	53	0.0	0.0
7	20030	A	0	9.0	25.7	0.2	0	33	0.0	0.0
7	20030	B	1	6.0	4.8	1.1	43	25	0.0	0.0
7	20030	C	0	6.6	7.2	0.7	32	26	0.0	0.0
7	20030	D	0	1.9	7.1	0.0	0	57	0.0	0.0
7	20030	E	0	3.4	7.5	0.2	0	53	0.0	0.0
7	20030	F	0	5.3	15.4	0.1	5	30	0.0	0.0
7	20040	A	0	11.0	13.1	0.8	22	24	0.0	0.0
7	20050	A	0	5.9	6.0	0.7	5	57	0.0	0.0
7	20050	B	0	9.0	10.2	0.8	0	54	0.0	0.0
7	20050	C	0	7.7	10.0	0.6	1	49	0.0	0.0
7	20050	D	0	3.9	10.4	0.1	0	45	0.0	0.0
7	20050	E	0	6.8	27.0	0.1	0	40	0.0	0.0
7	20050	F	0	8.0	37.1	0.1	0	37	0.0	0.0
7	20060	A	0	14.0	30.8	0.3	0	42	0.0	0.0
7	20060	B	0	11.7	38.3	0.2	0	43	0.0	0.0
7	20060	C	0	8.1	23.9	0.2	0	44	0.0	0.0
7	20070	A	0	2.4	11.3	0.0	0	46	0.0	0.0
7	20070	B	0	3.8	8.6	0.2	0	49	0.0	0.0
7	20070	C	0	7.8	12.9	0.4	1	43	0.0	0.0
7	20080	A	1	11.0	10.6	1.1	18	33	0.0	0.0
7	20080	B	0	3.3	3.6	0.5	41	33	0.0	0.0

Estimated depth may be unreliable because the stronger part
of the conductor may be deeper or to one side of the flight
line, or because of a shallow dip or overburden effects.

HUCKLEBERRY MTN. (AREA 3)

FLIGHT	LINE	ANOMALY	CATEGORY	AMPLITUDE (PPM) INPHASE	QUAD.	CTP MHOS	CONDUCTOR DEPTH MTRS	BIRD HEIGHT MTRS		
7	20090	A	4	2.0	0.3	8.3	74	52	0.0	0.0
7	20100	A	0	5.9	5.4	0.9	0	67	0.0	0.0
7	20110	A	0	4.7	12.8	0.1	0	47	0.0	0.0
7	20110	B	0	0.6	2.6	0.0	23	36	0.0	0.0
7	20130	A	0	13.0	17.6	0.7	0	44	0.0	0.0
7	20140	A	0	2.1	12.5	0.0	0	52	0.0	0.0
7	20140	B	0	-2.5	3.5	0.0	0	50	0.0	0.0
7	20140	C	0	-3.6	3.9	0.0	0	47	0.0	0.0
7	20140	D	0	3.1	10.5	0.0	0	43	0.0	0.0
7	20140	E	0	8.7	20.5	0.2	0	40	0.0	0.0
7	20140	F	0	13.9	39.2	0.2	0	38	0.0	0.0
7	20140	G	0	6.5	17.9	0.2	0	37	0.0	0.0
7	20140	H	1	4.8	3.9	1.0	38	35	0.0	0.0
7	20140	J	0	2.7	2.6	0.6	49	35	0.0	0.0
7	20150	A	0	5.3	8.4	0.4	12	39	0.0	0.0
7	20150	B	0	5.9	15.9	0.2	5	30	0.0	0.0
7	20170	A	0	5.6	11.5	0.2	6	37	0.0	0.0
7	20180	A	0	15.2	26.3	0.5	0	43	0.0	0.0
7	20180	B	0	5.2	6.4	0.5	8	51	0.0	0.0
7	20180	C	0	6.7	17.8	0.2	0	49	0.0	0.0
7	20200	A	0	4.5	12.1	0.1	0	50	0.0	0.0
7	20200	B	0	7.6	42.6	0.0	0	40	0.0	0.0
7	20200	C	0	8.6	56.7	0.0	0	44	0.0	0.0
7	20210	A	0	4.0	14.5	0.1	0	48	0.0	0.0
7	20210	B	0	1.5	10.3	0.0	0	49	0.0	0.0
7	20220	A	0	10.6	33.2	0.2	0	28	0.0	0.0
7	20220	B	0	14.5	41.6	0.2	0	26	0.0	0.0
7	20220	C	0	0.1	12.9	0.0	0	27	0.0	0.0
7	20220	D	0	2.4	20.6	0.0	0	37	0.0	0.0
7	20220	E	0	1.3	19.1	0.0	0	48	0.0	0.0
7	20220	F	0	2.2	16.8	0.0	0	45	0.0	0.0
7	20230	A	0	2.8	2.0	0.9	0	118	0.0	0.0
7	20230	B	0	2.1	6.2	0.0	0	81	0.0	0.0

Estimated depth may be unreliable because the stronger part
of the conductor may be deeper or to one side of the flight
line, or because of a shallow dip or overburden effects.

HUCKLEBERRY MTN. (AREA B)

FLIGHT	LINE	ANOMALY	CATEGORY	AMPLITUDE (PPM)		CONDUCTOR	CTP DEPTH	BIRD HEIGHT		
				INPHASE	QUAD.	MHOS	MTRS	MTRS		
7	20230	C	0	-2.3	11.9	0.0	0	42	0.0	0.0
7	20230	D	0	-1.4	20.1	0.0	0	42	0.0	0.0
7	20250	A	0	2.0	11.6	0.0	0	35	0.0	0.0
7	20250	B	0	2.2	3.5	0.2	34	36	0.0	0.0
7	20250	C	0	0.3	14.0	0.0	0	29	0.0	0.0
7	20250	D	0	2.9	12.9	0.0	7	26	0.0	0.0
7	20310	A	0	2.0	10.2	0.0	0	206	0.0	0.0

APPENDIX III

## CERTIFICATE OF QUALIFICATION

I, Roderick W. Woolham of the town of Pickering, Province of Ontario, do hereby certify that:-

1. I am a geophysicist and reside at 1463 Fieldlight Blvd., Pickering, Ontario, L1V 2S3

2. I graduated from the University of Toronto in 1961 with a degree of Bachelor of Applied Science, Engineering Physics, Geophysics Option. I have been practising my profession since graduation.

3. I am a member in good standing of the following organizations: The Association of Professional Engineers of the Province of Ontario (Mining Branch); Society of Exploration Geophysicists; South African Geophysical Association.

4. I have not received, nor do I expect to receive, any interest, directly or indirectly, in the properties or securities of New Canamin Resources Ltd. or any affiliate.

5. The statements contained in this report and the conclusions reached are based upon evaluation and review of maps and information supplied by Geonex Aerodat.

6. I consent to the use of this report in submissions for assessment credits or similar regulatory requirements.

R. W. Woolham, P.Eng.

Pickering, Ontario

October 8, 1993
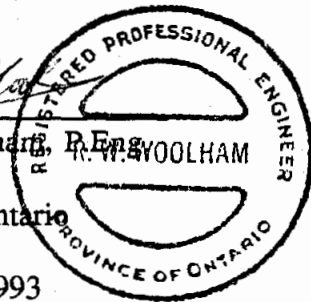
APPENDIX IV

PERSONNEL

FIELD

Flown	July 2 to 7, 1993
Pilot(s)	L. Stanley
Operator(s)	L. Moore

OFFICE

Processing	Pierre Marchand George McDonald
Report	R. W. Woolham

RSGM ——————————————————————————————————❖
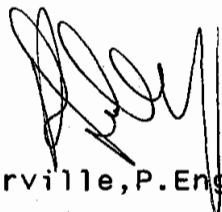
APPENDIX #2

COST STATEMENT
STATEMENT OF WORK

COST STATEMENT – AREA A

Geonex Aerodat	$32,100.00
Fuel (helicopter)	$ 4,198.77
Camp (3 men @ $50/day for 7 days plus GST)	$ 1,123.50
Drafting (12 hrs @ $20/hr plus GST)	$ 256.80
Report	$ 1,605.00
SUBTOTAL	$39,284.07
Less Tournagain Mining Area	($ 6,297.50)
Less Area B	($ 7,940.54)
TOTAL COSTS AREA A	$25,046.54

The above constitutes a true cost statement of the costs involved in the Airborne Geophysical Survey over Area A.

·R.Somerville,P.Eng.